

<https://doi.org/10.1016/j.jenvman.2022.115295>

This item is likely protected under Title 17 of the U.S. Copyright Law. Unless on a Creative Commons license, for uses protected by Copyright Law, contact the copyright holder or the author.

Access to this work was provided by the University of Maryland, Baltimore County (UMBC) ScholarWorks@UMBC digital repository on the Maryland Shared Open Access (MD-SOAR) platform.

Please provide feedback

Please support the ScholarWorks@UMBC repository by emailing scholarworks-group@umbc.edu and telling us what having access to this work means to you and why it's important to you. Thank you.



Review

Advanced oxidation processes: Performance, advantages, and scale-up of emerging technologies

Monali Priyadarshini^a, Indrasis Das^{b,c,*}, Makarand M. Ghangrekar^{a,c}, Lee Blaney^{d,**}^a School of Environmental Science and Engineering, Indian Institute of Technology, Kharagpur, West Bengal, 721302, India^b Environmental Engineering Department, CSIR-Central Leather Research Institute, Adyar, Chennai, Tamil Nadu, 600020, India^c Department of Civil Engineering, Indian Institute of Technology Kharagpur, Kharagpur, West Bengal, 721302, India^d Department of Chemical, Biochemical, and Environmental Engineering, University of Maryland Baltimore County, Baltimore, MD, 21250, USA

ARTICLE INFO

Keywords:

Advanced oxidation process
Contaminants of emerging concern
Emerging technologies
Mineralization
Process scale-up
Reaction mechanism

ABSTRACT

Advanced oxidation processes (AOPs) are promising technologies for partial or complete mineralization of contaminants of emerging concern by highly reactive hydroxyl, hydroperoxyl, superoxide, and sulphate radicals. Detailed investigations and reviews have been reported for conventional AOP systems that have been installed in full-scale wastewater treatment plants. However, recent efforts have focused on the peroxymonosulphate, persulphate, catalytic ozonation, ultrasonication and hydrodynamic cavitation, gamma radiation, electrochemical oxidation, modified Fenton, and plasma-assisted AOPs. This critical review presents the detailed mechanisms of emerging AOP technologies, their performance for treatment of contaminants of emerging concern, the relative advantages and disadvantages of each technology, and the remaining challenges to scale-up and implementation. Among the evaluated technologies, the modified electrochemical oxidation, gamma radiation, and plasma-assisted systems demonstrated the greatest potential for successful and sustainable implementation in wastewater treatment due to their environmental safety, compatibility, and efficient transformation of contaminants of emerging concern by a variety of reactive species. The other emerging AOP systems were also promising, but additional scale-up trials and a deeper understanding of their reaction kinetics in complex wastewater matrices are necessary to determine the technical and economic feasibility of full-scale processes.

Authors' contributions

Monali Priyadarshini: Literature review; Information collection; Writing - original draft. Indrasis Das: Conceptualization; Writing - original draft; Writing - review & editing. Lee Blaney: Writing - review & editing. M. M. Ghangrekar: Funding acquisition; Project administration; Writing - review & editing.

1. Introduction

The occurrence of pseudo-persistent organic contaminants, such as

dyes, pharmaceuticals, pesticides, and endocrine disrupting chemicals, in the aquatic environment poses serious threats to humans and aquatic organisms (Priyadarshini et al., 2020). The removal or transformation of these contaminants in wastewater is currently a high priority to avoid their discharge into receiving waters. Conventional treatment techniques, such as adsorption, coagulation, and ultrafiltration, only change the phase of these organic contaminants and do not transform them into benign compounds (Adak et al., 2019). Biological treatment strategies are relatively ineffective due to the bio-recalcitrant nature of trace organic contaminants (Mota et al., 2009; Priyadarshini et al., 2021a, 2021b; Titchou et al., 2021a). To overcome these challenges, advanced

Abbreviations: AOP, Advanced oxidation process; BDD, Boron-doped diamond; BOD, Biochemical oxygen demand; C₀, Initial concentration; COD, Chemical oxygen demand; e_{aq}⁻, Hydrated electron, EAOP, Electrochemical advanced oxidation process, EF, electro-Fenton, FeS₂ -, Pyrite, Fe²⁺; Ferrous ion, γ, Gamma, H, Hydrogen atom, HC, Hydrodynamic cavitation, HO₂, Hydroperoxyl radical; H₂O₂, Hydrogen peroxide; NHE, Normal hydrogen electrode; •OH, Hydroxyl radical; O₂⁻, Superoxide radical, O[•], Oxygen atom, PMS, Peroxymonosulfate, PS, Persulfate, R, Organic pollutant, R[•], Active organic radical, SR-AOPs, Sulphate radical based AOP, SO₄⁻, Sulphate anion radical; TOC, Total organic carbon; US, Ultrasound; USA, United States of America; USD, United States dollar; UV, Ultraviolet.

* Corresponding author. Environmental Engineering Department, CSIR-Central Leather Research Institute, Adyar, Chennai, Tamil Nadu, 600020, India.

** Corresponding author.

E-mail addresses: indrasis@clri.res.in (I. Das), blaney@umbc.edu (L. Blaney).

<https://doi.org/10.1016/j.jenvman.2022.115295>

Received 20 February 2022; Received in revised form 3 May 2022; Accepted 10 May 2022

Available online 18 May 2022

0301-4797/© 2022 Elsevier Ltd. All rights reserved.

oxidation processes (AOPs) have demonstrated the potential for rapid degradation of toxic contaminants in wastewater.

The AOPs are efficient techniques to produce reactive species, such as hydroxyl radicals ($\cdot\text{OH}$), hydroperoxyl radicals ($\text{HO}_2\cdot$), sulphate radicals ($\text{SO}_4^{\cdot-}$) and superoxide anion radicals ($\text{O}_2^{\cdot-}$) (Wang and Xu, 2012). These free radicals are highly reactive due to their unpaired electrons and have demonstrated the ability to degrade organic contaminants. The AOPs have been primarily classified according to the method of radical generation, namely chemical, photochemical, radiation-induced, cavitation, and electrochemical. The most widely investigated AOP technology is the Fenton process, which was originally observed as oxidation of tartaric acid in the presence of ferrous salt (Fenton, 1894). This concept was further modified to involve activation of hydrogen peroxide (H_2O_2) by ferrous ions (Fe^{2+}) to form $\cdot\text{OH}$ (Haber and Weiss, 1932). The efficiency of the Fenton process was enhanced by irradiation with ultraviolet (UV) or solar light (Ruppert et al., 1993). Other AOPs, including heterogeneous photocatalysis (e.g., TiO_2 , ZnO , Fe_2O_3) and ozone-based systems (e.g., O_3/UV , $\text{O}_3/\text{H}_2\text{O}_2$, $\text{UV}/\text{H}_2\text{O}_2/\text{O}_3$), have also been well-documented for the degradation of organic contaminants (Adak et al., 2019, 2015; Blaney et al., 2019; Chen et al., 2019; Hitam and Jalil, 2020; Priyadarshini et al., 2021a, 2021b; Ratshiedana et al., 2021; Rosenfeldt et al., 2006; Senthilnathan and Philip, 2010; Tamimi et al., 2006; Vinet and Zhedanov, 2011; Wu et al., 2019).

As of April 2022, about 16,865 articles on AOPs were available in the Scopus database. Some of these reports have indicated the high cost of conventional $\cdot\text{OH}$ -based AOPs due to high energy consumption, which is widely considered the major weakness of these treatment systems (Khan et al., 2020). To overcome this drawback, emerging technologies, such as $\text{SO}_4^{\cdot-}$ (Guerra-Rodríguez et al., 2018), electrochemical oxidation (Sirés et al., 2014), cavitation (Gevari et al., 2020), and radiation-induced (Rahman and Hung, 2019) AOPs, have been proposed for degradation of organic contaminants in wastewater.

2. Review focus and novelty statement

A rigorous review of AOP literature from 2010 to 2022 was performed, with a specific focus on emerging AOP technologies; however, some articles published before 2010 were also collected to explain advanced oxidation mechanisms and contextualize AOP performance. These articles were identified by searching for the following keywords in the Elsevier, Springer, Google Scholar, and Scopus databases: “advanced oxidation process”; “advanced oxidation process + wastewater treatment”; “emerging contaminants”; “field scale + advanced oxidation process”; and, “pilot scale + advanced oxidation process”. Overall, 237 peer-reviewed articles, books, and book chapters were used to develop this critical review. Previous reviews on AOPs (Table S1 in the Supporting Information (SI)) highlighted the reaction mechanisms, factors affecting performance, and lab-scale application of conventional AOP technologies. In addition, a few articles also summarized the reaction kinetics, performance, and practical challenges associated with AOPs (Cuerda-Correa et al., 2019; Lin et al., 2022; Oturan and Aaron, 2014; Rayaroth et al., 2022; Salimi et al., 2017). However, the mechanisms of emerging AOPs, status of field-scale applications, advantages and disadvantages of scale-up and commercialization, recent modifications of conventional technologies, and latest advancements in the field of AOPs have not been addressed in previous reviews. This critical review addresses these knowledge gaps.

3. Conventional and emerging AOP technologies

Comprehensive reviews of conventional AOPs, including O_3/UV , $\text{O}_3/\text{H}_2\text{O}_2$, $\text{UV}/\text{H}_2\text{O}_2$, Fenton, and electrochemical oxidation processes, are available in the literature (Fig. 1) (Asghar et al., 2015; Deng and Zhao, 2015; Fast et al., 2017; Giwa et al., 2021; Khan et al., 2020; Khare et al., 2021; Krishnan et al., 2021; Lin et al., 2022; Oturan and Aaron, 2014; Poyatos et al., 2010; Rayaroth et al., 2022; Tufail et al., 2021; Wang and Xu, 2012). In this critical review, emerging AOPs and novel

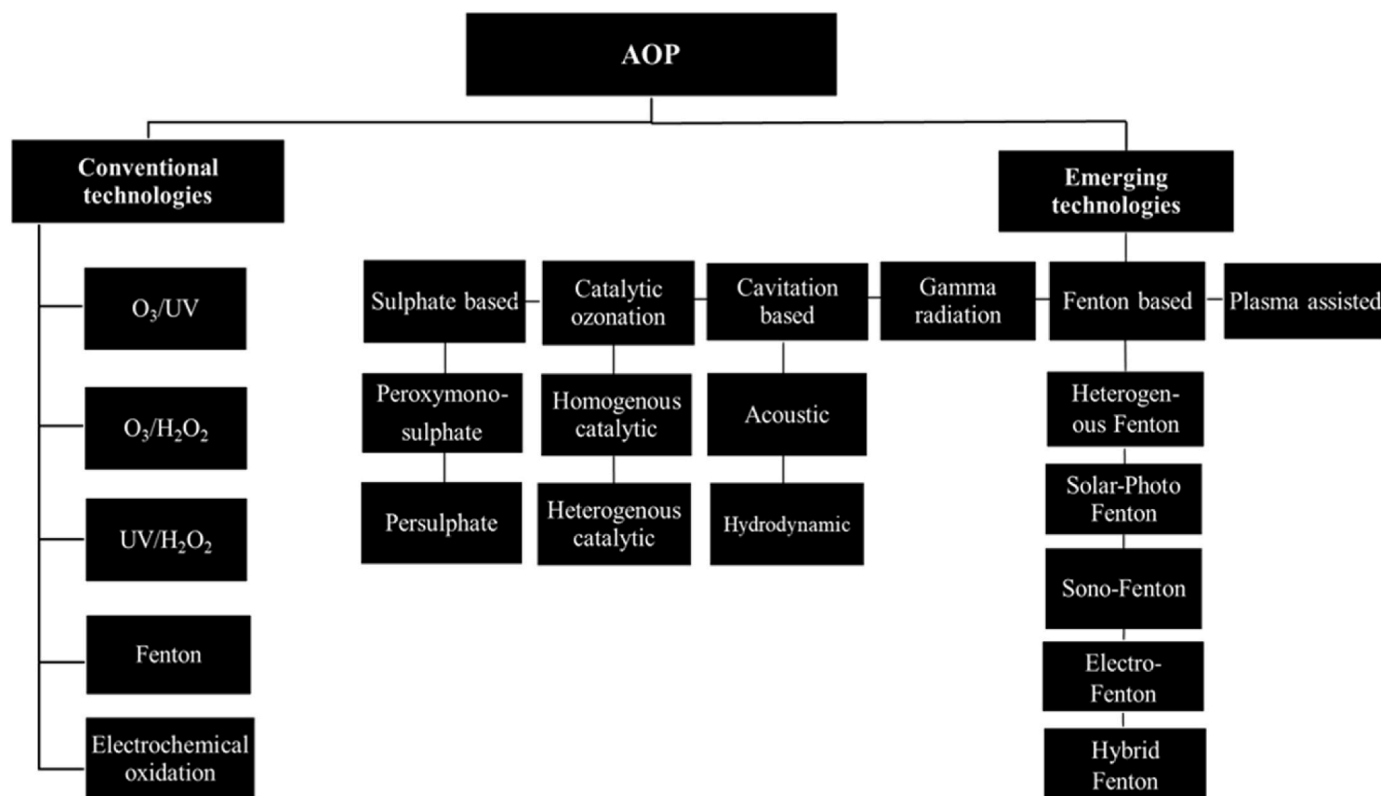


Fig. 1. Classification of conventional and emerging AOP-based technologies.

modifications to conventional AOPs have been identified from articles published after 2010. Most of the corresponding research was limited to bench-scale experiments; however, a few investigations were conducted with pilot- or full-scale processes in real wastewater treatment plants (He et al., 2020a, 2020b; Rodríguez-Chueca et al., 2018, 2019). The following sections describe the detailed mechanisms, advantages, disadvantages, and performance of emerging AOP technologies at the bench-, pilot-, and full-scale.

4. Peroxymonosulphate- and persulphate-based AOPs

Sulphate radical-based AOPs (SR-AOPs) are promising technologies, in which peroxymonosulphate (PMS, HSO_5^-) or persulphate (PS, $\text{S}_2\text{O}_8^{2-}$) salts are used as precursors to form highly reactive $\text{SO}_4^{\bullet-}$ for degradation of organic contaminants in wastewater (Anipsitakis and Dionysiou, 2003; Guerra-Rodríguez et al., 2018). The PMS and PS salts are 2 × cheaper than H_2O_2 , which is often used for production of $\bullet\text{OH}$ in conventional AOPs (Duan et al., 2015; Wacławek et al., 2017). Unlike $\bullet\text{OH}$, $\text{SO}_4^{\bullet-}$ exhibits high selectivity for reaction with organic contaminants in wastewater, a major advantage of this technology (Duan et al., 2015; Wacławek et al., 2017). Furthermore, $\text{SO}_4^{\bullet-}$ demonstrates a competitive oxidation potential (2.5–3.1 V_{NHE}) compared to $\bullet\text{OH}$ (1.8–2.7 V_{NHE}) (Hu and Long, 2016). The higher oxidation potential of $\text{SO}_4^{\bullet-}$ facilitates efficient degradation of complex organic compounds (Zhang et al., 2020).

Different energy sources, such as heat (Huang et al., 2021), ultrasound (US) (Deng et al., 2015), UV light (Antoniou et al., 2010), and gamma radiation (Alkhuraji et al., 2017), have been adopted to activate PMS and PS to generate $\text{SO}_4^{\bullet-}$ (Fig. 2) by two main pathways: (1) homolytic cleavage of O–O bonds (Eq. 1–2); and, (2) water dissociation into H^\bullet and $\bullet\text{OH}$, followed by H^\bullet reaction with PS and PMS (Eq. 3–5).

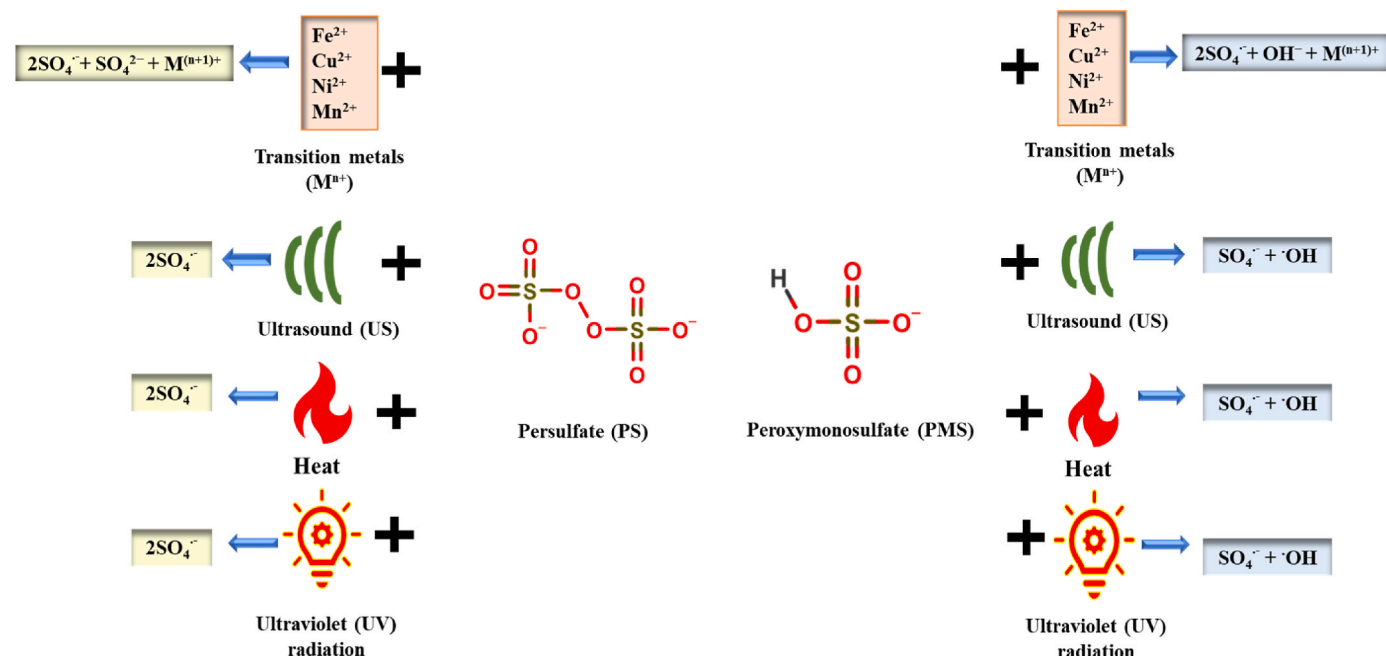


Fig. 2. Different activation methods for sulphate-based AOPs.

SR-AOPs have been proven to be promising technologies for wastewater treatment (Zhang et al., 2015). The performance of SR-AOPs can be enhanced through incorporation of heterogeneous catalysts. For example, 26 mg L^{-1} of N-doped porous carbon and 3.5 mM of PMS efficiently transformed 40 μM of losartan (antihypertensive drug) in wastewater and achieved almost 70% mineralization within 4 h of treatment (De Andrade et al., 2020). Similarly, over 97% degradation of 50 μM of acid red 1 (dye) was observed within 10 min by activating PMS with a NaBO_2 catalyst at neutral pH (Rao et al., 2020). For environmentally-relevant conditions, the UV/PMS system achieved almost complete degradation of 200 ng L^{-1} of sulfamerazine (antibiotic) within 30 min by employing 80 mJ cm^{-2} of UV fluence (Cui et al., 2016). Almost 70% of 50 μM of tyrosol (antioxidant) was effectively degraded at pH 6.8 by UV/PMS treatment with a fluence of 640 mJ cm^{-2} (Kilic et al., 2019). In a similar study, ~100% degradation of 20 mg L^{-1} of rhodamine B (dye) was achieved within 30 min by the MoFe/TiO_2 solar light-activated PMS process (Dong et al., 2021).

PS-based AOPs were also effective for degradation of contaminants of emerging concern. For example, a nano-scale, zero-valent iron and PS-based Fenton system achieved approximately 96% degradation of 50 mg L^{-1} sulfamerazine in wastewater within 30 min (Wu et al., 2020a, 2020b). The CuS/PS /visible light system was employed for treatment of 60 mg L^{-1} orange II (dye), and 98.9% transformation was achieved within 2 h (Zhu et al., 2020). Similarly, rusted waste iron particles ($\text{Fe}^0/\text{Fe}_x\text{O}_y$) activated PS to achieve 95% degradation of 200 μM of orange II within 2 h (Yu et al., 2020). In another report, approximately 90% degradation of 100 μM cephalosporin (antibiotic) was achieved within 4 h using 1 mM of PS at neutral pH (Qian et al., 2020). Other investigations involving PMS- and PS-based treatment of contaminants of emerging concern in wastewater are summarized in Table 1.

4.1. Advantages and disadvantages of SR-AOPs

The efficient performance of SR-AOP technologies has been reported over a wide pH range of 2.0–8.0 (Zhang et al., 2015, 2022). $\text{SO}_4^{\bullet-}$ selectively attacks aromatic or unsaturated π bonds in organic contaminants, generating intermediate products and, eventually, fully mineralized end products (e.g., CO_2 , H_2O). Alternatively, $\bullet\text{OH}$ are non-selective oxidants that react by hydrogen abstraction or

Table 1
Removal efficiency of emerging contaminants by SR-AOPs.

AOP	Contaminant	C ₀ (mg L ⁻¹)	Time (min)	Experimental conditions	Efficiency (%)	Reference
Light/PMS	Di-(2-ethylhexyl) phthalate	10	70	UV fluence = 63 mJ cm ⁻² PMS = n.a. ^a	90	Huang et al. (2017)
Light/PMS	Ciprofloxacin	16.6	60	UV fluence = n.a. ^a PMS = 1 mM	97	Mahdi-Ahmed and Chiron (2014)
Light/PMS	Sulfamerazine	2 × 10 ⁻⁴	30	UV fluence = 77 mJ cm ⁻² , PMS = 1 mg L ⁻¹	~100	Cui et al. (2016)
Light/PMS	Tyrosol	6.9	n.a. ^a	UV fluence = 640 mJ cm ⁻² PMS = 1 mg L ⁻¹	70	Kilic et al. (2019)
Light/PMS/Fe ³⁺	4-chlorophenol	12.9	60	UV fluence = n.a. ^a PMS = 1 mM Fe ³⁺ = 1 mM	~100	Hasan et al. (2020)
Light/PMS/Activated carbon fiber-supported ferric alginate	Azophloxine	25.5	24	UV fluence = n.a. ^a PMS = 5 mM Catalyst = 2 g L ⁻¹	~100	Wu et al. (2020a, 2020b)
PMS/N-doped Carbon	Losartan	18.4	240	PMS = 3.5 mM Catalyst = 26 mg L ⁻¹	70	De Andrade et al. (2020)
PMS/NaBO ₂	Acid red 1	25.5	10	PMS = 3.5 mM Catalyst = 26 mg L ⁻¹	97	Rao et al. (2020)
Light/PS	Chloramphenicol	10	60	UV fluence = 9 mJ cm ⁻² PS = 0.25 mM	~100	Ghauch et al. (2017)
Light/PS/Rectorite sludge derived biochar supporting ZnO	Acid Orange 7	20	180	UV fluence = n.a. ^a PS = 2 mM Catalyst = 0.9 g L ⁻¹	85	Guan et al. (2020)
Light/PS/ZnO/CuBi ₂ O ₄	Rhodamine B	4.8	120	UV fluence = n.a. ^a PS = 1.48 mM Catalyst = 0.1 g L ⁻¹	80	Sabri et al. (2020)
Light/PS/CuS	Orange II	60	120	UV fluence = n.a. ^a PS = 100 mg L ⁻¹ Catalyst = 15 mg L ⁻¹	98.88	Zhu et al. (2020)
PS/Fe@ granular red mud reinforced by zero-valent iron (GRM)	Acid orange 7	1000	120	PS = 500 mM Catalyst = 1 g L ⁻¹	90.8	Du et al. (2020)
PS/Mg doped CuO-Fe ₂ O ₃	Phenol	33	45	PS = 0.2 g L ⁻¹ Catalyst = 0.6 g L ⁻¹	84.4	Sun et al. (2020)
PS/Nano zero-valent iron	Sulfamerazine	50	30	PS = 1 mM Catalyst = 2 mM	96	Wu et al. (2020a, 2020b)
PS/Fe ⁰ @Fe _x O _y	Orange II	70	120	PS = 2 mM Catalyst = 2 g L ⁻¹	95	Yu et al. (2020)
PS/organo-montmorillonite supported nano-zero valent iron	Sulfamethazine	20	10	PS = 4 mM Catalyst = 1.5 mM	97	Wu et al. (2019)
PS/US	Naphthol blue black	5	20	PS = 1 g L ⁻¹ US frequency = 20 kHz	95	Ferkous et al. (2017)

a: n.a., not available; C₀: the initial contaminant concentration.

electrophilic addition mechanisms (Liang and Bruell, 2008). The half-life of SO₄^{•-} is 30–40 μs, about 1500–2000 times longer than that of •OH (20 ns), reinforcing the higher stability of SO₄^{•-} and emphasizing the better opportunities for controlled design and performance of SR-AOPs (Ghanbari and Moradi, 2017). As noted above, SO₄^{•-} also possesses a higher oxidation potential than •OH (Xia et al., 2020).

Although SR-AOPs exhibit several advantages over •OH-based technologies, one obvious limitation is the increase in sulphate, which is an end product of PMS and PS decomposition, content in treated waters. The high sulphate concentrations in treated wastewater may warrant additional polishing steps, such as precipitation, ion exchange, nano-filtration, reverse osmosis, or biological degradation (Zhang et al., 2015). In addition, activation of PMS and PS in SR-AOPs exerts a large energy demand in the form of heat, UV light, or US, raising important considerations for process sustainability and scale-up (Duan et al., 2020).

4.2. Scale-up of SR-AOPs

An SR-AOP process was scaled-up for tertiary treatment in the Estivel wastewater treatment plant in Toledo, Spain (Rodríguez-Chueca

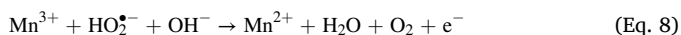
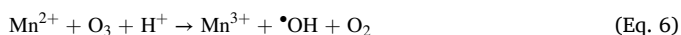
et al., 2018, 2019). Approximately 12,000 m³ d⁻¹ of wastewater was treated using a UV-C driven SR-AOP to degrade antibiotics and antimicrobial resistance genes present in the wastewater (Rodríguez-Chueca et al., 2018, 2019). Preliminary economic assessments were conducted based on the cost of installation and operation, and the PMS/UV-C and PS/UV-C AOPs were more economical than the H₂O₂/UV-C system (Rehman et al., 2018; Xiao et al., 2016). In another study, solar photocatalysis with 200 mg L⁻¹ TiO₂ and 0.125 mM PS achieved complete degradation of 1 mg L⁻¹ trimethoprim in the presence of 10 mg L⁻¹ of humic acid using a 39-L pilot-scale plant at Plataforma Solar de Almería, Spain (Grilla et al., 2019). A 1000-L solar-driven, heat-activated PS reactor was applied for treatment of ten different types of pharmaceuticals in wastewater effluent from southwestern Europe (Telegang Chekem et al., 2020). Of the ten pharmaceuticals, only caffeine and tramadol were present at trace levels after 2 h of treatment at 70 °C with 200 μM PS (Telegang Chekem et al., 2020). Nevertheless, UV-, US-, heat-, and radiation-based activation of PS and PMS involve tremendous energy demands, necessitating analysis of the energy and cost requirements for activation systems prior to process scale-up.

5. Recent modifications to ozone-based AOPs

When operated under certain conditions, ozonation is a promising AOP (Text S2 in SI). Recent work has demonstrated that O_3 combined with H_2O_2 and UV light can enhance the rate of contaminant degradation due to rapid $\cdot OH$ production (Tichonovas et al., 2017; Xia and Hu, 2018). However, ozone-based processes have several drawbacks, including the high energy consumption to produce O_3 gas, slow mass transfer of O_3 from the gaseous to aqueous phase, low solubility of O_3 in water at environmental temperature, the instability of O_3 in solution, and low oxidation efficiency for some contaminants due to the selective nature of O_3 reactions (Xiong et al., 2018). To overcome these challenges, catalytic ozonation processes have been developed for water and wastewater treatment of contaminants of emerging concern. In general, the catalytic ozonation processes are classified into two categories, namely homogenous and heterogeneous, depending upon the catalyst properties (Pirgalioğlu and Özbelge, 2009).

5.1. Homogeneous catalytic ozonation process

In homogenous catalytic ozonation processes, dissolved metals, such as Zn^{2+} , Mn^{2+} , Co^{2+} , Cu^{2+} , and Fe^{3+} , are used to catalyze O_3 decomposition reactions and produce $\cdot OH$ and $HO_2\cdot$, according to Eq. 6–9 (Huang et al., 2016). A specific catalyst dose is required for optimal performance of the catalytic ozonation processes. Catalyst doses above the optimum condition can lead to excessive $\cdot OH$ scavenging, decreasing the process efficiency for transformation of contaminants of emerging concern (Wu et al., 2008).



The efficiency and feasibility of homogenous catalytic ozonation processes have been reported for degradation of organic contaminants in wastewater. For example, $100 \mu g L^{-1}$ acetamidiprid (model compound) was treated with the O_3/Fe^{2+} system, and 50% degradation was achieved within 60 min for an O_3 concentration of $10 mg L^{-1}$ and a catalyst dose of $10 mg L^{-1}$ (Malvestiti et al., 2019). Similar efforts identified the successful mineralization of amoxicillin by the $O_3/UV/Fe^{2+}$ process,

which outperformed O_3 and O_3/Fe^{2+} (Gotvajin et al., 2021). In the presence of Fe^{2+} and UV radiation, 93.4% degradation of amoxicillin was achieved within 120 min; however, removal efficiencies of 75.7% and 89.8% were observed for O_3 and O_3/Fe^{2+} treatment, suggesting presence of Fe^{2+} and UV radiation enhanced the catalytic effect for the transformation of amoxicillin in the $O_3/UV/Fe^{2+}$ process (Gotvajin et al., 2021). The above findings demonstrate the feasibility of homogenous catalytic ozonation processes, but the main drawback of these systems is the addition of metal ions that requires further downstream treatment or recovery (Pines and Reckhow, 2002).

5.2. Heterogeneous catalytic ozonation process

To overcome the drawbacks of homogenous catalytic ozonation, solid catalysts with high stability and efficiency have been developed. In particular, metal oxide (e.g., TiO_2 , MnO_2 , Al_2O_3) and metal/metal oxide supports (e.g., $Cu-TiO_2$, $Cu-Al_2O_3$, $Re-CeO_2$) have been employed as heterogeneous catalysts to activate O_3 decomposition reactions and transform organic contaminants (Beltrán et al., 2003). The interactions between the catalysts, organic contaminants, and O_3 include three possible scenarios (Fig. 3). The primary reaction scheme involves adsorption and decomposition of O_3 molecules on the catalyst surface to form free radicals, which then react with organic contaminants in the water phase (Eq. 10–13, where S represents a surface site on the catalyst). In the second scenario, organic contaminants adsorb to the catalyst surface and are oxidized by O_3 . The third situation involves adsorption of both O_3 and the organic contaminants on the surface prior to reaction (Wang and Chen, 2020).



The performance of heterogeneous catalytic ozonation processes has been well reported in the literature (Table S2 in the SI). For example, 99.3% transformation of $100 mg L^{-1}$ of 4-nitrophenol (phenolic compound) was achieved after 45 min of treatment by the MnO_2/O_3 system ($100/50 mg L^{-1}$) at pH 5.9 (Nawaz et al., 2017). Similarly, catalytic ozonation of $50 mg L^{-1}$ of 1-amino-4-bromoanthraquinone-2-sulfonic

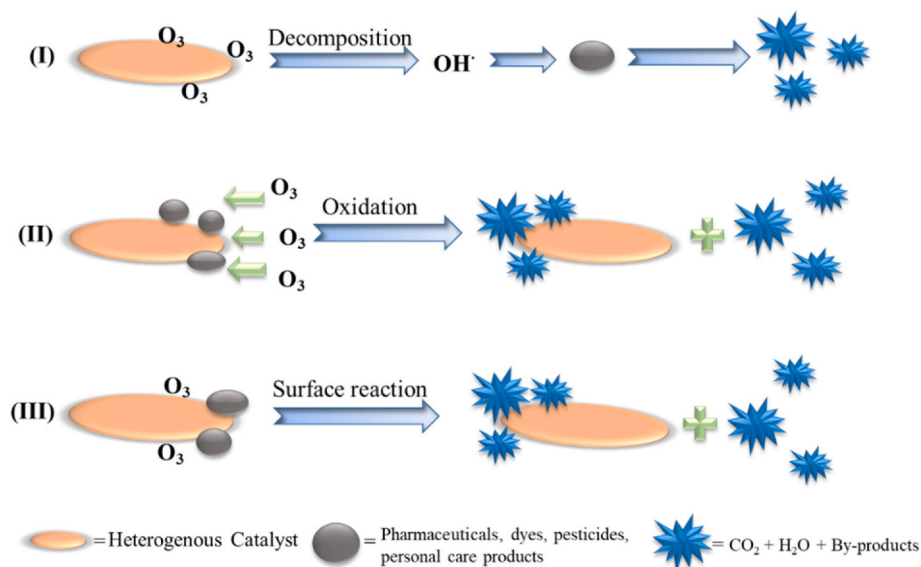


Fig. 3. Three mechanisms for degradation of organic contaminants by heterogeneous catalytic ozonation processes.

acid (precursor of dyes) was evaluated with an alumina-supported, Mn–Ce-mixed oxide catalyst ($\text{Mn-CeO}_x/\text{Al}_2\text{O}_3$); almost complete removal was observed after 120 min of treatment with 20 mg L^{-1} of O_3 and 1 g L^{-1} of catalyst. Importantly, only 32.7% transformation of 1-amino-4-bromoanthraquinone-2-sulfonic acid was achieved with O_3 alone (Wu et al., 2018). Within 30 min of treatment, 79.9% degradation of acid red 183 (dye) was achieved in a solar catalytic ozonation process with 5 mg L^{-1} of Al_2O_3 and 0.9 mg min^{-1} of O_3 at pH of 7.0 (Ikhlaiq et al., 2021).

5.3. Advantages and disadvantages of catalytic ozonation

Catalytic ozonation processes maintain several advantages over conventional ozone-based AOPs. Because UV light (e.g., O_3/UV) and pH adjustment (e.g., O_3/HO^-) are not required, the operating costs are lower for catalytic ozonation. Coupling ozone and heterogeneous catalysis can enhance the reaction kinetics, improve O_3 utilization efficiency, and reduce the time required to achieve complete mineralization of contaminants of emerging concern in wastewater (Malik et al., 2020). The remaining challenges to widespread adoption of catalytic ozonation processes include selection of efficient and cost-effective catalysts, development of efficient regeneration and reuse protocols, preventative strategies to control catalyst leaching, and assessment of residual toxicity in treated wastewater to confirm process sustainability (Mecha and Chollom, 2020). More detailed discussion of catalyst regeneration protocols and leaching control strategies was provided by Argyle and Bartholomew (2015) and Zhao et al. (2020).

5.4. Scale-up of catalytic ozonation systems

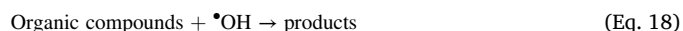
Laboratory-scale investigations of catalytic ozonation have been well-documented for the degradation of organic contaminants; however, only a few reports have evaluated the commercial applicability of catalytic ozonation processes. In particular, a 222-m^3 catalytic ozonation reactor was used to treat $100 \text{ m}^3 \text{ h}^{-1}$ of effluent from a biologically-treated coking wastewater. The chemical oxygen demand (COD) of the effluent was 195 mg L^{-1} , and 45.6% COD removal was observed after 90 min of treatment with 180 g L^{-1} of $\text{Mn}_x\text{Ce}_{1-x}\text{O}_2/\gamma\text{-Al}_2\text{O}_3$ catalyst and 80 mg L^{-1} of O_3 (He et al., 2020a, 2020b). A 2.93-m^3 pilot-scale catalytic ozonation process was operated for treatment of $22 \text{ m}^3 \text{ h}^{-1}$ of biologically-treated dyeing and finishing wastewater with $132\text{--}148 \text{ mg L}^{-1}$ of COD. The system achieved 69% COD removal after 30 min of treatment with a zero-valent iron catalyst and 120 mg L^{-1} of O_3 (Ma et al., 2018). In addition, a 100-L pilot-scale reactor was used to treat real textile effluent from a Konark Industry facility in Kolhapur, India. The system accomplished 90% COD removal after 30 min of treatment with 40 mg L^{-1} of O_3 and 2 g L^{-1} of Cu-doped ZnO catalyst (Nakhate et al., 2019). Economic assessments were also conducted to compare the total costs per 1000 L treated, and the catalytic ozonation system (United States dollar (\$) 3.8) was cheaper than US (\$) 75, O_3 (\$) 9.6 and $\text{O}_3/\text{H}_2\text{O}_2$ (\$) 7.1 (Nakhate et al., 2019).

6. Cavitation-based AOPs

The production of $\bullet\text{OH}$ through cavitation (Text S3 in the SI) is classified into four categories: acoustic cavitation or ultrasonication; hydrodynamic cavitation (HC); particle cavitation; and, optic cavitation. Acoustic cavitation or ultrasonication uses ultrasonic frequencies between 16 and 100 kHz to generate microbubbles (Chowdhury and Viraraghavan, 2009). The microbubbles are formed by velocity or pressure variations caused by flowing water in specially-designed HC systems (Kumar et al., 2000). In particle and optic cavitation processes, cavities are produced by proton beams or other photon sources in bubble producing chambers (Futakawa et al., 2007; Lauterborn, 1979). Among the different systems, acoustic cavitation and HC are the most promising technologies for oxidation of dissolved organic chemicals due to

straightforward operation and efficient generation of reactive species (Gagol et al., 2018).

The primary degradation mechanism of organic molecules by cavitation processes involves two steps: (i) production of highly reactive $\bullet\text{OH}$ by splitting water molecules and dissolved oxygen as presented in Eq. 14–17; and, (ii) reaction of $\bullet\text{OH}$ with organic contaminants in wastewater (Eq. (18)) (Salimi et al., 2017). The production of reactive species can be further enhanced by introducing O_3 , which thermally decomposes within the microbubbles to form $\bullet\text{OH}$ and $\text{O}_2^{\bullet-}$ (Eq. 19–21). Subsequently, $\bullet\text{OH}$ can react with organic contaminants by attacking aromatic rings or aliphatic chains (Kang and Hoffmann, 1998).



6.1. Acoustic cavitation/ultrasonication

The acoustic cavitation process involves ultrasonic waves that cause a series of compression and rarefaction cycles, which are responsible for the expansion and implosive collapse of bubbles or cavities in wastewater. The sudden collapse of bubbles or cavities releases energy at extremely high temperature ($>5000 \text{ K}$) and pressure ($>1000 \text{ bar}$), facilitating the degradation of organic contaminants (Ashokkumar, 2011; Bang and Suslick, 2010; Miklos et al., 2018). Acoustic cavitation may occur through physical (direct) or chemical (indirect) mechanisms. Physical acoustic cavitation involves the formation and collapse of microbubbles by ultrasonic waves, as described above. In chemical acoustic cavitation, water or dissolved oxygen undergo homolytic fragmentation to produce reactive species, such as $\bullet\text{OH}$, HO_2^\bullet , and O^\bullet , which then degrade organic contaminants (Gevari et al., 2020). The formation of $\bullet\text{OH}$ by indirect ultrasonication can be enhanced through combination with other processes, including US/O_3 , $\text{US}/\text{H}_2\text{O}_2$, $\text{US}/\text{O}_3/\text{H}_2\text{O}_2$, and $\text{US}/\text{photocatalysis}$ (Babu et al., 2016).

In recent years, acoustic cavitation has been investigated for degradation of contaminants of emerging concern. Following 40 min of treatment with US at 20 kHz and 20 mg L^{-1} H_2O_2 , near complete degradation of $200 \mu\text{M}$ hexabromocyclododecane (flame retardant) was achieved (Panda et al., 2020). The treatment of olive mill wastewater was evaluated with the $\text{US}/\text{UV}/\text{TiO}_2$ system, and 59% of COD removal was observed after 90 min (Al-Bsoul et al., 2020). A combination of sonolysis at 24 kHz and hexagonal magnesium oxide anchored with carbon nanotubes was employed to degrade 45 mg L^{-1} sulfadiazine (antibiotic) in wastewater to concentrations below the detection limit within 80 min (Hayati et al., 2020). Other researchers have also reported the successful application of acoustic cavitation, suggesting that this technology is a promising and efficient wastewater treatment process (Table S3 in the SI).

6.2. Hydrodynamic cavitation

In hydrodynamic cavitation or HC, microbubbles are generated by the passage of liquid through a mechanical constriction, such as an orifice plate or a specially designed reactor. When the liquid passes through the orifice, the pressure at the constricted point increases the

kinetic energy of the liquid and simultaneously drops below the vapour pressure, causing the formation of microbubbles (Dular et al., 2016). The microbubbles subsequently undergo growth and implosive collapse, releasing large amounts of energy that can degrade contaminants (Jyoti and Pandit, 2001). Importantly, hydrodynamic reactors are simple and easy to operate, because the primary equipment is a centrifugal pump. To further increase the treatment efficiency, the reactor can be designed to include UV and H₂O₂ modules upstream or downstream of the cavitation reactor (Gagol et al., 2018).

The unique and eco-friendly properties of HC for production of reactive species in wastewater have received attention in recent years. For example, efficient degradation of 20 mg L⁻¹ 2,4,6-trichlorophenol (herbicide) was achieved by coupling HC with O₃ and H₂O₂. The 2,4,6-trichlorophenol degradation efficiencies reached ~100% and 95.5% for the HC/O₃/H₂O₂ and O₃/H₂O₂ systems, respectively, after 120 min of treatment with an inlet pressure of 4 bar (Barik and Gogate, 2018). Another effort used 2,4-dinitrophenol as a model organic contaminant to investigate the performance of the HC/FeSO₄/H₂O₂ and HC/Fe/H₂O₂ processes with an inlet pressure of 4 bar. Within 60 min, 20 mg L⁻¹ of 2,4-dinitrophenol was completely degraded by the HC/FeSO₄/H₂O₂ process, but only 54% degradation was achieved after 120 min treatment with the HC/Fe/H₂O₂ system (Bagal and Gogate, 2013). Other coupled HC systems have shown promising results for the transformation of contaminants of emerging concern in wastewater (Table S4 in the SI).

6.3. Advantages and disadvantages of cavitation-based AOPs

Compared to other AOPs, cavitation systems have several advantages, including the simple and flexible operation, minimal maintenance costs associated with the use of standard equipment, and low mass transfer resistance due to the formation of microcirculation and turbulence zones in the reactor (Jyoti and Pandit, 2001). However, cavitation-based AOPs also involve certain drawbacks that may prevent full-scale implementation, such as the uneven distribution of cavitation effects and need for additional oxidants, such as H₂O₂ and O₃, to enhance process efficiency. For hydrodynamic cavitation systems, expensive pumps are necessary to achieve the high operating pressures. In acoustic cavitation processes, the relatively large volume of wastewater can absorb ultrasonic waves generated by the sonic transducers, decreasing cavitation efficiency and generation of •OH. Acoustic cavitation is also more efficient under acidic pH conditions; therefore, pH swings may be required to optimize performance and, subsequently, neutralize the treated wastewater (Gevvari et al., 2020).

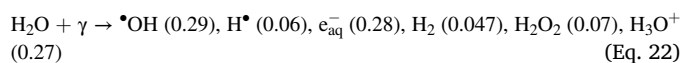
6.4. Scale-up of cavitation-based AOPs

Cavitation-based AOPs have been identified as promising technologies for wastewater treatment because of their simple operation and efficient generation of reactive species. Bench- and pilot-scale investigations of acoustic cavitation systems have been successful; however, full-scale applications have not yet been reported (Ashokkumar, 2011; Jing et al., 2017; Manickam et al., 2014; Papoutsakis et al., 2015). In contrast, several pilot-scale installations with HC processes have been operated (Joshi and Gogate, 2019; Kovacic et al., 2020; Pradhan and Gogate, 2010; Zampeta et al., 2021). A 22-L hybrid HC and photocatalytic pilot-scale system was used to degrade 100 mg L⁻¹ of reactive red 180 dye in wastewater, and the system achieved 60% mineralization after 180 min of treatment with 1 g L⁻¹ of ZnO loading under 5 bar inlet pressure (Çalışkan et al., 2017). One full-scale, HC-based AOP was also operated to treat 54–163 m³ d⁻¹ of wastewater containing methyl tert-butyl ether (gasoline additive) from the March Air Force Base in Riverside, California (USA) (Kommineni et al., 2000). The system achieved an 80% decrease in methyl tert-butyl ether concentration. A few investigations have provided economic assessments of cavitation-based technologies, but the results suggested the need for further reductions in

energy requirements and chemical consumption to attain competitive processes (Choi et al., 2019; Gagol et al., 2019; Thanekar et al., 2020).

7. Gamma radiation-based AOPs

Gamma-ray irradiation causes radiolysis of water ($t \leq 10^{-12}$ s; Eq. (22)) and produces highly reactive •OH oxidants and strong reducing species, such as hydrated electrons (e_{aq}^-) and hydrogen atoms (H•), without the need for exogenous chemicals or catalysts (Alkharaji et al., 2017; Capodaglio, 2020). The values in the parentheses of Eq. (22) indicate the radiation yield (G-value, $\mu\text{mol J}^{-1}$), which corresponds to the number of molecules, atoms, or free radicals produced or consumed per 100 eV of absorbed energy (Rauf and Ashraf, 2009). The •OH production can be further improved by adding H₂O₂ (Eq. (23)) to enhance mineralization of contaminants of emerging concern (Iqbal and Bhatti, 2015; Melo et al., 2008). The reactive species generated in Eq. 22–23 can effectively degrade organic contaminants in wastewater.



Gamma ray-based AOPs have been successfully employed to degrade pesticides, dyes, organic contaminants, and pharmaceuticals in wastewater (Wang and Xu, 2012). For example, 25 kGy gamma radiation was combined with 38 mM of H₂O₂ to treat 50 mg L⁻¹ of acid red 73 (dye) in wastewater, and 96.3% degradation was achieved (Jamil et al., 2020). Ganguli et al. investigated the effects of graphene oxide addition on the degradation of 20 mg L⁻¹ phenol under gamma irradiation. With 8 kGy of gamma radiation and 1.54 g L⁻¹ of graphene oxide, 98.8% degradation of phenol was observed in 30 min (Ganguli et al., 2020). In another study, near complete degradation of 100 μM diclofenac (anti-inflammatory) was attained with 25 kGy gamma radiation and 1 mM N₂O, while 81% mineralization of diclofenac was achieved with 1 mM of H₂O₂ in the same system (Alkharaji, 2019). The authors indicated that reduction reactions between e_{aq}^- and N₂O increased the yield of •OH to a greater extent than in the H₂O₂ system. Other promising investigations have also reported the transformation of contaminants of emerging concern by gamma radiation-based AOPs in laboratory-scale reactors (Table S5 in the SI).

7.1. Advantages and disadvantages of gamma radiation-based AOPs

Compared to other technologies, gamma radiation AOPs are advantageous due to the high penetration of gamma rays in wastewater (unlike UV and acoustic sonication), lack of sludge formation, and high reaction rates achieved by the variety of reactive species generated during operation (e.g., Eq. (22)). The major drawbacks of gamma radiation-based AOPs are the high energy requirement and need for skilled technicians and protective equipment, which increase the operating and capital costs (Weber, 2002).

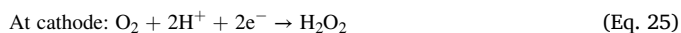
7.2. Scale-up of gamma radiation-based AOPs

Only a few investigations have explored the commercial application of gamma radiation-based AOPs for wastewater treatment. For example, a 1000 m³ d⁻¹ pilot plant with sequential 1–2 kGy ionizing radiation and biological treatment processes was installed to treat wastewater from an industrial textile dyeing manufacturer in Daegu, Korea (Han et al., 2002). The system achieved a considerably increase in (more than 30%) degradation of harmful organic impurities under the optimum electron-beam absorbed dose of 1 kGy and electron beam power of 400 kW. Following the successful pilot-scale operation, an industrial wastewater treatment plant was constructed to treat up to 10,000 m³ d⁻¹ of wastewater. The capital and operating costs of this facility were 4 and 0.5 million \$ per year, respectively, which translated to 0.3 \$ per

1000 L of wastewater or 50% of the cost for conventional treatment processes (Han et al., 2012). Promising economics have also been reported for wastewater treatment with the combined gamma/H₂O₂ and gamma/K₂S₂O₈ AOPs (Changotra et al., 2019; Chmielewski, 2006).

8. Recent modifications to electrochemical AOPs

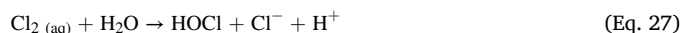
Electrochemical AOPs (EAOPs) are clean and effective technologies that produce [•]OH via direct or indirect mechanisms (Oturán and Brillas, 2007). The direct oxidation system involves electrochemical production of [•]OH without the addition of exogenous chemicals; in particular, water molecules are oxidized at the anode surface and H₂O₂ is produced at the cathode surface (Eq. 24–25) (Nidheesh and Gandhimathi, 2012). A number of chemical reagents have been evaluated to enable indirect oxidation mechanisms in EAOPs (Text S5 in the SI) (Martínez-Huitle and Ferro, 2006). Light and US irradiation have been combined with EAOPs to increase production of reactive species (Hiller et al., 1992; Pelegrini et al., 2000; Skoumal et al., 2009). Although electrochemical oxidation is a conventional technology, hybrid systems, such as the electro-Fenton process and electrochemical oxidation with Cl₂, have provided new opportunities for effective treatment of contaminants of emerging concern (Ahmadzadeh and Dolatabadi, 2018).



8.1. Electrochemical generation of chlorine-based reactive species

The electrochemical generation of Cl₂ reactive species offers effective pathways for combined disinfection and degradation of organic contaminants in wastewater (Sirés et al., 2014). Initially, Cl₂ forms by the oxidation of Cl[−] at the anode surface (Eq. (26)). Then, Cl₂ reacts with H₂O to produce HOCl and Cl[−] via disproportionation reactions (Eq. (27)). HOCl undergoes acid dissociation to form OCl[−] (Eq. (28)), with the extent of OCl[−] production being dependent on the solution pH. The HOCl is reactive and known to oxidize biorefractory contaminants present in wastewater (García-Segura et al., 2018). Sánchez-Montes et al. (2020) examined this EAOP through application of a boron-doped diamond (BDD) anode for treatment of 50 mg L^{−1} glyphosate (herbicide), and complete degradation was achieved with a current density of 10 mA cm^{−2} and 2 g L^{−1} of NaCl. In another study, 89.6%, 92.6%, 99.6% degradation of acetaminophen (analgesic), diclofenac, and sulfamethoxazole, respectively, was achieved through electrogenerated [•]OH and reactive chlorine species (e.g., Cl[•], Cl₂^{•−}, ClO[•]) produced through graphite electrode (Liu et al., 2019). Additional examples of

EAOPs are summarized in Table 2.



8.2. Advantages and disadvantages of EAOPs

In general, EAOPs use fewer chemicals than other AOPs to produce reactive species capable of degrading organic contaminants. EAOPs can also be effectively operated over a wide range of solution pH, require shorter reaction times, and do not produce waste sludge (Brillas and Sirés, 2015; Titchou et al., 2021b). The electrochemical generation of H₂O₂ via cathodic reduction of O₂ reduces the costs and risks associated with handling, transportation, and storage of H₂O₂ (Zhang et al., 2019). Notable drawbacks of EAOPs are the high operational costs from electricity consumption, capital costs of the electrode materials, and maintenance issues stemming from electrode fouling. These concerns have prevented the sustainable application of EAOPs for treatment of real wastewater (Pikalova et al., 2019; Woisetschlager et al., 2013).

8.3. Scale-up of EAOPs

Despite the large number of reports on laboratory-scale EAOPs, practical applications are still scarce. A 0.25 L s^{−1} pilot-scale catalytic electrochemical system was used to treat produced wastewater, and the system achieved 90% of BOD and COD removal efficiencies after 6 min with an active metal (M)/C/Fe cathode and 120 A of current (Ma and Wang, 2006). Only one article has addressed the commercial use of EAOPs for disinfection of real swimming pool water (Naji et al., 2018). The performance of the electrochemical system was evaluated for niobium-doped BDD (Nb/BDD) and titanium-coated platinum (Ti/Pt) anodes. Using the Nb/BDD (1.5 A current) and Ti/Pt (3.0 A current) anodes, 100 L of swimming pool water, which initially contained 10⁶ colony-forming units per 100 mL, was almost completely inactivated (i.e., approximately six-log inactivation). These results highlight the promising disinfection performance of EAOPs, but additional pilot- and full-scale studies are necessary to confirm treatment efficacy for contaminants of emerging concern. Additional research is required to fabricate low-cost, but effective, electrodes for use in pilot-scale systems to inform opportunities for full-scale EAOP implementation.

9. Recent modifications to fenton and photo-fenton AOPs

Fenton-based technologies are the most convenient and extensively investigated AOPs for treatment of organic contaminants in wastewater.

Table 2
Degradation of emerging contaminants by EAOPs.

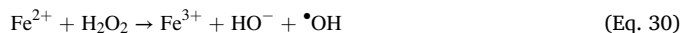
Anode	Contaminant	C ₀ (mg L ^{−1})	Experimental conditions	Current density (mA cm ^{−2})	Efficiency (%)	Reference
BDD	Ofloxacin	36.1	FeSO ₄ •7H ₂ O = 0.1 mM Time = 480 min	9.37	~100	Yang et al. (2020)
BDD	Propranolol	154	FeSO ₄ •7H ₂ O = 0.5 mM Time = 420 min	40	~100	Isarain-Chávez et al. (2010)
Dimensionally stable anode	Imatinib	34.5	FeSO ₄ •7H ₂ O = 0.1 mM Time = 480 min	16.66	~100	Yang et al. (2019)
RuO ₂ -TiO ₂ /Ti	<i>p</i> -nitrophenol	50	NaCl = 0.05 M Time = 60 min	100	~100	Wang et al. (2020)
Graphite	Cytarabine	20	NaCl = 0.05 M Time = 60 min	10	98	Sivodia and Sinha (2020)
BDD	2,4-dichloro-phenoxyacetic acid	99.4	S ₂ O ₈ ^{2−} = 0.02 M Time = 10 min	20	70	Cai et al. (2018)
Graphite-PVC composite	Caffeine	5	NaCl = 0.06 M Time = 30 min	–	90	Al-Qaim et al. (2015)

The conventional Fenton process employs Fe^{2+} and H_2O_2 to generate $\bullet\text{OH}$ at low pH (Miller et al., 2017). This process involves a number of drawbacks: (i) large amounts of iron salt and H_2O_2 are necessary, which increases the operating costs; (ii) additional polishing units are required to remove iron from the process effluent, which increases capital and operating costs; (iii) a large quantity of iron-laden sludge is produced, posing challenges to appropriate waste management; and (iv) the efficacy of the process decreases at neutral pH, increasing operating complexity and costs (He et al., 2020a, 2020b). To overcome these shortcomings and improve treatment efficacy in real wastewater matrices, modifications to the conventional Fenton process have been investigated (Fig. 4).

9.1. Heterogeneous Fenton processes

Heterogeneous Fenton processes use solid catalysts containing iron-based minerals in place of dissolved Fe^{2+} (Kaviya, 2020). In the conventional Fenton process, the consumption of Fe^{2+} increases over time; however, heterogeneous Fenton processes extend catalyst life by minimizing the leaching of iron from the solid catalysts (Nidheesh, 2015). Ferrihydrite, goethite, hematite, magnetite, pyrite, and other iron minerals have been evaluated as catalysts for degradation of contaminants of emerging concern in wastewater. Alternative sources of iron, including clays, laterite, and industrial wastes (e.g., pyrite ash, electric arc furnace dust, fly ash, blast furnace dust), have also been deployed in modified Fenton processes (Zhang et al., 2019). Current research has prioritized immobilization of iron and iron oxides on different support materials, such as activated carbon, alumina, clay, mesoporous silica, and zeolites (Arimi, 2017; Hassan and Hameed, 2011). The supports allow deposition of iron (nano)particles with high surface area to prevent attrition of solid catalysts and reduce iron leaching into solution. The formation of reactive species by heterogeneous Fenton processes

involves a complex series of reactions at the catalyst surface, as indicated in Eq. 29–32 (Araujo et al., 2011).



In the last decade, development of low-cost, efficient, and accessible materials has been prioritized for heterogeneous Fenton processes. An Fe_2O_3 /carbon composite was employed for heterogeneous Fenton treatment of textile wastewater, and 71% of COD removal was achieved within 60 min using 300 g L^{-1} catalyst and 500 mg L^{-1} of H_2O_2 (Dantas et al., 2006). Another study used 100 mg L^{-1} of $\alpha\text{-FeOOH}$ nanorods to catalyze degradation of 80 mg L^{-1} methyl orange (dye), and 98% degradation was observed after 60 min (Liu et al., 2018). A novel catalyst was synthesized from natural zeolite for treatment of molasses distillery wastewater via heterogeneous Fenton reactions, and 90% decolorization and 60% of total organic carbon (TOC) removal were reported for operation with 150 g L^{-1} catalyst and 2 g L^{-1} H_2O_2 (Arimi, 2017). Similar outcomes from other heterogeneous Fenton processes are summarized in Table S7 of the SI.

Considering the challenges associated with the conventional Fenton process, heterogeneous Fenton technologies offer a number of advantages for treatment of contaminants of emerging concern, including applicability across a wide pH range, less iron leaching, low sludge production, and high catalyst stability and reusability (Mahmoodi et al., 2019). However, the introduction of heterogeneous Fenton technologies in wastewater treatment plants has been inhibited by a number of drawbacks, such as high chemical requirements and complicated

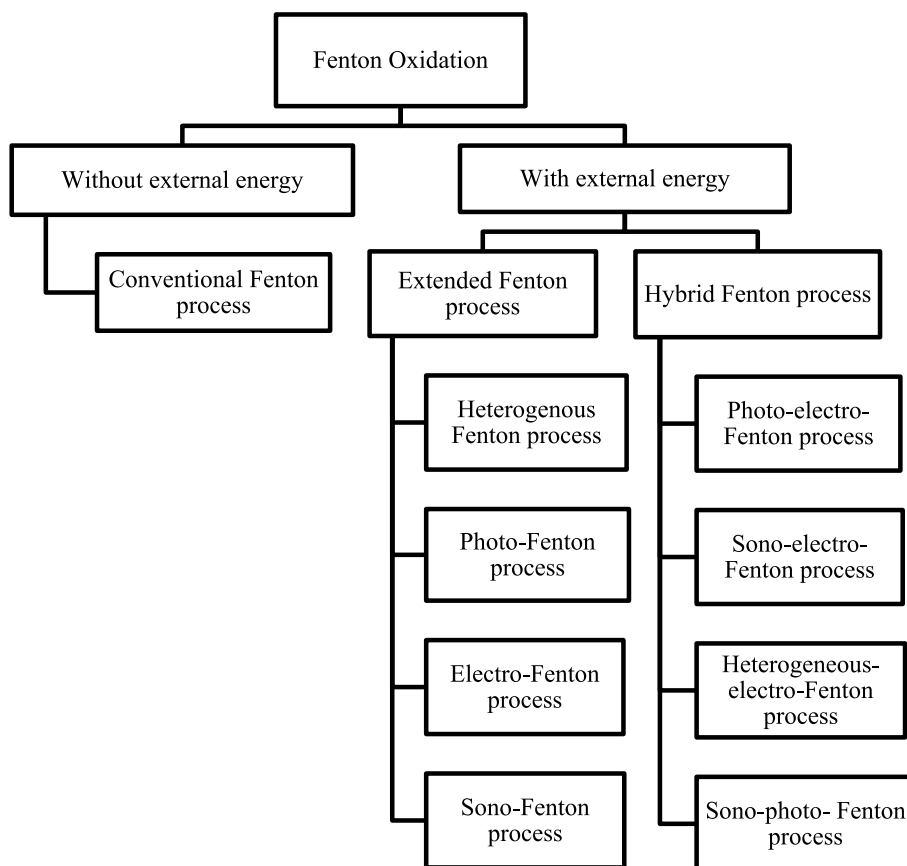


Fig. 4. Classification of modified Fenton processes.

synthesis protocols associated with novel catalysts (Ganiyu et al., 2018).

9.2. Photo-Fenton processes

Introduction of UV or visible light to the Fenton process improves the production of $\bullet\text{OH}$ and, therefore, enhances the degradation of contaminants of emerging concern (Wang et al., 2016). The improved performance of the photo-Fenton process stems from accelerated reduction of Fe^{3+} to Fe^{2+} , which then reacts with H_2O_2 to generate $\bullet\text{OH}$ and Fe(III) as the $[\text{FeOH}]^{2+}$ complex. Under light irradiation, the $[\text{FeOH}]^{2+}$ complex undergoes a charge transfer process to efficiently regenerate the Fe^{2+} ions and restart the cycle (Eq. (33)). Furthermore, direct photolysis of H_2O_2 simultaneously produces $\bullet\text{OH}$, according to Eq. (34) (Mishra et al., 2017).

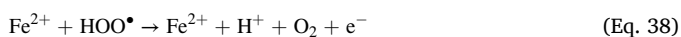
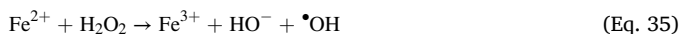


The photo-Fenton process has been extensively investigated with solar, visible, and UV light sources and found to exhibit high performance, energy efficiency, and process versatility (Table S7 in the SI). A comparative evaluation of the conventional Fenton and UV-Fenton processes was undertaken for treatment of adsorbable organic halides in pulp and paper industry wastewater. Almost 95% transformation of the adsorbable organic halides was achieved within 10 min by adding 2.0 mM Fe^{2+} into the UV-Fenton system, whereas only 85% transformation was attained with 8.5 mM Fe^{2+} in the conventional Fenton process (Ribeiro et al., 2020). Another study identified the optimal experimental conditions, namely 20 mg L^{-1} of Fe^{2+} and 100 mg L^{-1} of H_2O_2 , for a visible light assisted photo-Fenton process that exhibited 59% mineralization of 4-octylphenol, 4-nonylphenol, bisphenol A, estrone, 17 β -estradiol, 17 α -ethinylestradiol, and estriol (Silva et al., 2021). Casierri-Martinez et al. (2020) evaluated the solar-photo-Fenton process for treatment of 15 $\mu\text{g L}^{-1}$ diclofenac and 15 $\mu\text{g L}^{-1}$ carbamazepine in domestic wastewater, and 92% and 86% mineralization efficiencies were achieved, respectively, within 66.5 min of treatment.

Compared to conventional Fenton processes, the photo-Fenton system is advantageous due to (i) lower chemical consumption from the use of light to activate H_2O_2 and (ii) lower production of iron-laden sludge (Pliego et al., 2015; Sánchez Pérez et al., 2013). However, the photo-Fenton process involves higher capital and operating costs from the lamps, decreased performance at neutral pH, and the complicated design of photoreactors, all of which pose challenges to full-scale operation (Wang et al., 2016).

9.3. Sono-Fenton processes

The rapid degradation of contaminants of emerging concern by the sono-Fenton process provides an effective alternative to conventional Fenton systems. As explained in Section 6, the rapid formation, growth, and collapse of microbubbles or cavities releases a large amount of energy and produces reactive species, such as $\text{H}\bullet$, $\bullet\text{OH}$, and $\text{HO}_2\bullet$ (Wojnárovits and Takács, 2008). The combination of US with the Fenton process considerably improved performance compared to the individual systems (Pliego et al., 2015) due to enhanced production of $\bullet\text{OH}$ from recovered Fe^{2+} (Eq. 35–39) (Bagal and Gogate, 2014).



The benefits of the US-Fenton process have been widely reported

(Table S7 in the SI). For example, the sono-Fenton system was adopted for degradation of 200 mg L^{-1} of 2,4-dichlorophenol (precursor of herbicide) in wastewater, and 77.9% degradation was observed within 140 min for the following operating conditions: 35 kHz US frequency, 400 mg L^{-1} H_2O_2 dose, 10 mg L^{-1} Fe^{2+} loading, and pH of 5.0. Transformation of carbofuran (pesticide) was investigated with the US-Fenton process at 20 kHz. For an initial concentration of 20 mg L^{-1} carbofuran, more than 99% degradation and 40% mineralization were achieved within 30 min using 200 mg L^{-1} of H_2O_2 and 10 mg L^{-1} of Fe^{2+} (Ma and Sung, 2010). Similarly, complete degradation of 20 mg L^{-1} naproxen (anti-inflammatory) was observed within 10 min in the US-Fenton system with 59 kHz, 9.98 mM H_2O_2 , and 4.83 mg L^{-1} Fe^{2+} (Lan et al., 2012).

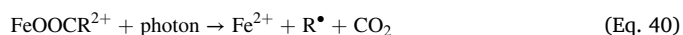
Overall, the sono-Fenton process is advantageous for wastewater treatment, because the generation of $\text{H}\bullet$, $\bullet\text{OH}$, and $\text{HO}_2\bullet$ can effectively enhance the degradation rate of organic contaminants (Bagal and Gogate, 2014). Mass transfer limitations are a major concern in Fenton processes, but these issues can be efficiently eliminated by creating mechanical turbulence via ultrasonic irradiation (Chowdhury and Viraraghavan, 2009). While promising, full-scale operations are still limited due to the challenges associated with distributing cavity formation throughout the reactor, high costs of operation, and practical issues involved with the design of large-scale cavitation reactors (Pliego et al., 2015).

9.4. Hybrid Fenton processes

Hybrid Fenton processes have been developed and investigated for treatment of contaminants of emerging concern. Due to their prevalence in the literature, the photo-electro-, sono-electro-, heterogeneous electro-, and sono-photo-Fenton processes are discussed in the following subsections.

9.4.1. Photo-electro-Fenton processes

The photo-electro-Fenton process enhances the production of $\bullet\text{OH}$ and, consequently, improves the degradation rate of contaminants of emerging concern. The photochemical regeneration of Fe^{2+} and direct photolysis of H_2O_2 improve the efficiency of the hybrid technology to produce $\bullet\text{OH}$ (Eq. 33–34) (Priambodo et al., 2011). Furthermore, ferric carboxylate complexes, such as ferric oxalate, which is a common byproduct of photo-electro-Fenton treatment, can enable additional transformation mechanisms through production of active organic radicals ($\text{R}\bullet$) (Eq. (40)) (Murillo-Sierra et al., 2018).



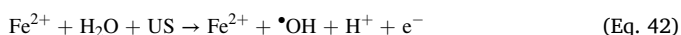
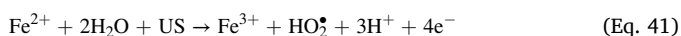
The effectiveness of the photo-electro-Fenton process has been successfully demonstrated for numerous contaminants (Table S7 in the SI). For example, a comparative evaluation of the coupled anodic oxidation and H_2O_2 (AO- H_2O_2), electro-Fenton, and solar photo-electro-Fenton processes was performed for treatment of 20 mg L^{-1} of TOC from the tebuthiuron and ametryn herbicides in wastewater. Approximately 70% mineralization was achieved after 6 h by the solar photo-electro-Fenton process with 0.5 mM Fe^{2+} and 50 mA cm^{-2} current density, while only 36% and 53% of TOC removal efficiencies were observed for the AO- H_2O_2 system and electro-Fenton process, respectively (Gozzi et al., 2017). Similarly, a 105 mg TOC L^{-1} mixture of the tartrazine, ponceau SS, and direct blue 71 dyes was treated by the AO- H_2O_2 , electro-Fenton, and solar photo-electro-Fenton processes. With 0.50 mM Fe^{2+} and 100 mA cm^{-2} current density, the solar photo-electro-Fenton process removed 99% of the TOC, outperforming the conventional electro-Fenton and AO- H_2O_2 systems by 1.8 and 18.3 times, respectively (Dos Santos et al., 2018).

The photo-electro-Fenton process exhibits three major advantages over conventional Fenton reaction chemistry: (i) the photo-electro-Fenton process is more effective for mineralization of contaminants of

emerging concern in real wastewater (Ganiyu et al., 2018); (ii) the quick regeneration of Fe^{2+} by photolysis of Fe^{3+} renders the process more efficient (Pliego et al., 2015); and, (iii) the light source reduces the need for expensive anodes (Pérez et al., 2017). Nevertheless, scale up of photo-electro-Fenton processes involves challenges from the capital and maintenance costs associated with UV lamps and maintaining acidic pH (Bagal and Gogate, 2014).

9.4.2. Sono-electro-Fenton process

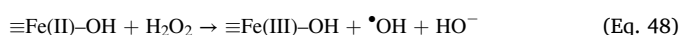
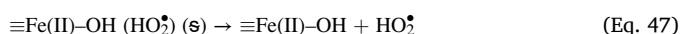
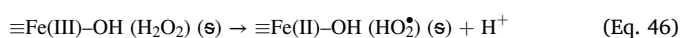
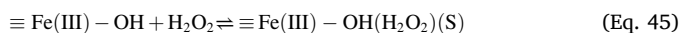
The degradation of contaminants of emerging concern by the sono-electro-Fenton process relies on both physical and chemical phenomena. The physical mechanisms relate to maintenance of fast mass transfer of contaminants to the electrode through mixing and regular electrode cleaning. The chemical reaction stems from the rapid collapse of microbubbles, which generate reactive species like $\cdot\text{OH}$ and $\text{HO}_2\cdot$, to degrade contaminants in wastewater (Eq. 41–42) (Ahmadi et al., 2019).



The performance of the sono-electro-Fenton treatment process has been rigorously investigated for nonbiodegradable contaminants (Table S7 in the SI). For example, saline petrochemical wastewater was treated by the PS- and US-based electro-Fenton processes. The results indicated that 94.1% of COD removal was achieved within 210 min for the US-electro-Fenton process with a sacrificial anode and graphite carbon cathode; 91.7% of COD removal was observed for the PS-electro-Fenton process with 0.75 mM PS and 1.2 V (Ahmadi et al., 2019). Degradation of 0.1 mM Meldola blue (dye) was investigated with a Pt gauze anode, reticulated vitreous carbon cathode, 124 kHz US frequency, and 0.5 mM Fe^{2+} , and the COD removal reached to 61% after 100 min of treatment (Abdelsalam and Birkin, 2002). The lower catalyst and chemical requirements, efficiency across a wide pH range, and rapid transformation kinetics for recalcitrant organics are major advantages of the sono-electro-Fenton process (Javaid and Qazi, 2019). However, this system also involves high energy consumption and operational costs; furthermore, treatment can increase the temperature of the process effluent, necessitating cooling stages before discharge to receiving waters (Moradi et al., 2020).

9.4.3. Heterogeneous electro-Fenton process

Stable solid catalysts, such as Fe-based bimetallic particles, goethite, magnetic chitosan beads, pyrite, and Y-zeolite, have been used as the iron source in heterogeneous electro-Fenton processes (Luo et al., 2020). Pyrite is the most abundant mineral in the earth's crust and contains a high fraction of iron, making it an excellent option for incorporation in heterogeneous electro-Fenton processes (Ouiriemmi et al., 2017). The governing reactions of this AOP are shown in Eq. 43–48 (Ganiyu et al., 2018; Wang et al., 2013).



The feasibility of heterogeneous electro-Fenton processes has been demonstrated for a variety of organic contaminants (Table S7 in the SI). For example, 1 g L^{-1} of chalcophyrite was used as a catalyst for transformation of 200 μM tetracycline in wastewater, and 98% mineralization was observed within 360 min using a BDD anode and carbon felt cathode (Barhoumi et al., 2017). The degradation of 100 μM acid orange

7 (dye) was evaluated with a CoFe-layered double hydroxide-modified carbon felt cathode and a heterogeneous catalyst. The TOC removal reached 60% after 2 h of treatment with a current density of 4.2 mA cm^{-2} (Ganiyu et al., 2017). The wide operating pH range, high catalyst stability and reusability, and enhanced production of reactive species are the main advantages of this technology (Thomas et al., 2021). The primary drawbacks of the heterogeneous electro-Fenton process include the high costs and negative environmental impacts of catalyst production (Labidh et al., 2015).

9.4.4. Sono-photo-Fenton process

The combination of US and light irradiation in the sono-photo-Fenton process generates the $\cdot\text{OH}$, $\cdot\text{OOH}$, and H^+ reactive species (Xu et al., 2014). During sonolysis, an appreciable amount of $\cdot\text{OH}$ and H^+ undergo recombination to form H_2O ; however, the incorporation of light prevents recombination reactions (Babuponnusami and Muthukumar, 2014) and also enables conversion of H_2O_2 to $\cdot\text{OH}$ (Eq. (49)). Otherwise, the reaction mechanisms involved in the sono-photo-Fenton process are similar to those described for the sono-Fenton process in Section 6.



A number of contaminants of emerging concern have been treated by the sono-photo-Fenton process (Table S7 in the SI). For example, this process was applied for treatment of phenolic wastewater with the Fe_2O_3 -SBA-15 heterogeneous catalyst. Almost 90% of the TOC was removed after 6 h of sonolysis with a 20 kHz frequency, whereas only 30% and 40% mineralization efficiencies were achieved by the Fenton and photo-Fenton systems, respectively (Segura et al., 2009). Another study employed the sono-photo-Fenton and TiO_2 photocatalysis processes for degradation of 39 μM ibuprofen. While 26% mineralization of ibuprofen was recorded for TiO_2 photocatalysis, 60% mineralization was attained for sono-photo-Fenton treatment with a 300 kHz US frequency (Méndez-Arriaga et al., 2009).

The major advantages of the sono-photo-Fenton process include the lower chemical and catalyst requirements, operational simplicity, wide pH tolerance, and compatibility with biological or physical treatment processes (Moradi et al., 2020). The principal concerns of sono-photo-Fenton treatment are the high energy consumption and the specialized reactor design required for incorporation of UV lamps, both of which increase the capital and operating costs (Yosofi and Mousavi, 2020).

9.5. Scale-up of the Fenton and modified-Fenton AOPs

The performance of Fenton and modified-Fenton processes has been well-documented for wastewater treatment at the laboratory-scale; however, pilot-scale applications have also been evaluated to determine commercial viability. For example, a 20-L solar photo-electro-Fenton reactor with a BDD anode and carbon-PTFE air-diffusion cathode achieved 90% mineralization of 50 mg L^{-1} sulfamethoxazole in wastewater after 6 h of operation with a current density of 47 mA cm^{-2} and a flow rate of 571 L h^{-1} (Murillo-Sierra et al., 2018). Similarly, a 250-L solar photo-Fenton pilot reactor was used to treat 600 L h^{-1} of secondary effluent containing 50 mg L^{-1} ofloxacin (antibiotic). The system, which was operated with 5 mg L^{-1} Fe^{2+} and 75 mg L^{-1} H_2O_2 , demonstrated 92.7% ofloxacin removal over 180 min of treatment. The preliminary economic analysis for a 150 $\text{m}^3 \text{d}^{-1}$ application of this system was found to be \$ 0.87 m^{-3} (Michael et al., 2012). A 10-L solar photo-Fenton pilot plant was constructed for treatment of petroleum refinery wastewater containing trace amounts of organic compounds like benzene, toluene, and ethylbenzene. After 180 min, the maximum COD (79.6%) and TOC (73.2%) removal efficiencies were achieved with 694.7 mg L^{-1} H_2O_2 , 67.3 mg L^{-1} Fe^{2+} , and pH of 3.2 (Pourehie and Saïen, 2020). In another study, the total operating cost of the solar photo-Fenton process was calculated to be \$ 10.4 m^{-3} , indicating that

the system was more economical than the solar/ $\text{ZnO}/\text{S}_2\text{O}_8^{2-}$ (\$ 30.74 m^{-3}) and solar/ $\text{TiO}_2/\text{S}_2\text{O}_8^{2-}$ (\$ 178.04 m^{-3}) processes for treatment of eight pesticides in drinking water (Fenoll et al., 2012; Pourehie and Saïen, 2020).

Pilot-scale operations have also investigated the degradation of other contaminants of emerging concern in Fenton and modified-Fenton treatment processes (Table 3) (Cabrera Reina et al., 2020). While the results are promising, the following issues must be addressed to improve the economics of Fenton-based wastewater treatment processes: (i) reduced production of iron-laden sludge; (ii) improved performance at environmentally relevant pH conditions; (iii) development of low-cost electrodes for electro-Fenton methods; and, (iv) decreased chemical demand. Future efforts are required to deconvolute contaminant degradation kinetics, synthesize highly stable and low-cost catalysts and electrode materials, and adopt renewable energy sources to power the treatment systems. These improvements will enable scale-up and commercialization of Fenton-based technologies.

10. Plasma-assisted AOPs

Due to the high transformation efficiency of organic contaminants, increased attention has been placed on environmentally compatible plasma-based AOPs. Plasma is a partially or fully ionized gas consisting of electrons, free radicals, and neutral species generated by electrical discharges. Plasma-based AOPs are generally categorized as thermal and non-thermal processes (Bogaerts et al., 2002). Thermal plasma, or equilibrium plasma, directly introduces a flux of high energy plasma-forming gas to wastewater by arc discharge, torches, or radio frequency. To do so, thermal plasma requires high temperatures ranging from 4000 to 20,000 K (Vandenbroucke et al., 2011). For non-thermal plasma, or non-equilibrium plasma, wastewater treatment is achieved by energetic electrons that react with background molecules, such as N_2 , O_2 , and H_2O , to produce secondary electrons and reactive species. The energetic electrons used in non-thermal plasma systems are generated by corona, gliding arc, spark, dielectric barrier, and glow discharges (Scholtz et al., 2015). Of these two techniques, the non-thermal plasma process has the most potential for implementation in wastewater treatment due to the lower power required for production of reactive species.

10.1. Formation of hydroxyl radicals in plasma-assisted AOPs

Electrical discharges generate charged plasma particles with 5–20 eV of energy. The charged particles can cause dissociation, ionization, and vibrational/rotational excitation of water molecules (Itikawa and Mason, 2005) to form the $\bullet\text{OH}$ and H^\bullet reactive species (Eq. 50–56).

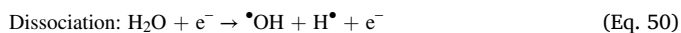
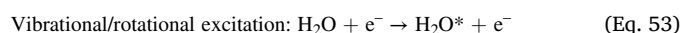


Table 3

Summary of the performance of pilot-scale Fenton and modified-Fenton processes for contaminant treatment.

Process	Contaminant	C_0 (mg L^{-1})	Experimental conditions	Removal efficiency (%)	Reference
Solar photo-electro Fenton	2,4-dichlorophen-oxyacetic acid	22×10^{-2}	Volume = 10 L Flow rate = 900 L h^{-1}	~100 ^c	Casado et al. (2006)
Sono-photo-Fenton	Oxalic acid	36×10^{-2}	Volume = 10 L Flow rate = 420 L h^{-1}	85 ^a	Papoutsakis et al. (2015)
Fenton oxidation	Bisphenol A	80	Volume = 2000 L Flow rate = 16,000 L h^{-1}	93 ^b	Gu et al. (2012)
Photo-Fenton	6-nitro-1-diazo-2- naphthol-4-sulfonic acid	7300 ^b	Volume = 37 L Flow rate = 14,000 L h^{-1}	80 ^a	De la Cruz et al. (2013)
Solar photo-Fenton	Effluent from a municipal wastewater treatment plant	7.5 ^a	Volume = 190 L	~100	Rodríguez et al. (2005)
Solar photo-Fenton	Phenol	0.1	Volume = 16 L Flow rate = 120 L h^{-1}	60 ^a	Arzate et al. (2020)
Solar photo-Fenton	Effluent from a municipal wastewater treatment plant	38×10^{-4a}			

a: as TOC; b: as COD; c: as contaminant degradation.



When oxygen is exposed to a high electrical discharge, the oxygen atom (O^\bullet) can be produced via O_2 dissociation. The oxygen atom can then react with (i) water to generate $\bullet\text{OH}$ (Eq. (57)) (Joshi and Thagard, 2013) and (ii) O_2 to produce O_3 (Eq. (58)). Introduction of H_2O_2 into the plasma system enables generation of $\bullet\text{OH}$ and $\text{O}_2^{\bullet-}$ (Eq. 59–60) (Staelin and Holgné, 1982). Plasma reactors can also be integrated with UV-based direct photolysis to increase the formation of $\bullet\text{OH}$ from H_2O_2 and O_3 (Anpilov et al., 2001). All of these reactive species can degrade contaminants of emerging concern in wastewater.



The application of non-thermal plasma AOPs has been widely investigated for the effective degradation of contaminants in wastewater. For example, a non-thermal gliding arc discharge with 2 g L^{-1} of TiO_2 photocatalyst was used to treat 80 μM of anthraquinonic acid green 25 dye in wastewater, and 93% of COD was removed after 60 min of treatment (Ghezzer et al., 2007). A multi-hole dielectric barrier discharge achieved 60% of COD removal from seaweed washing wastewater within 20 min (Ma et al., 2020). Treatment of 100 mg L^{-1} of chloroform and 100 mg L^{-1} of chlorobenzene was investigated by incorporating 3 g L^{-1} of TiO_2 - ZnO /granular activated carbon catalyst into a non-thermal pulsed corona discharge reactor, and near complete degradation was observed for both contaminants (Abedi et al., 2015). Several other promising reports of plasma-assisted AOP treatment systems are summarized in Table S8 of the SI.

10.2. Advantages and disadvantages of plasma-assisted AOPs

Plasma-assisted AOPs do not require costly chemicals but do involve safety hazards and generate toxic byproducts (Lesage et al., 2013; Vandenbroucke et al., 2011). The electrical discharges in water produce ions (e.g., H^+ , H_3O^+ , HO_2^\bullet , OH^\bullet), molecular species (e.g., H_2 , O_2 , H_2O_2), reactive radicals (e.g., O^\bullet , H^\bullet , $\bullet\text{OH}$, $\text{O}_2^{\bullet-}$), and intense shock waves, which can produce more $\bullet\text{OH}$ and H_2O_2 in the bulk liquid via dissociation of water molecules; these reactive species ultimately result in degradation of organic contaminants (Jiang et al., 2014; Reddy and Subrahmanyam, 2012). The major limitations associated with this

technology are the skilled labor desired to operate the plasma reactors and the high electrical energy requirement, both of which increase operating costs (Jiang et al., 2014).

10.3. Scale-up of plasma-assisted AOPs

The performance of pilot-scale, non-thermal plasma processes has been investigated for treatment of organic contaminants; however, no full-scale applications of this technology currently exist. A 150-L pilot plant was operated for degradation of pharmaceuticals and endocrine disrupting chemicals in wastewater from Upper Galilee, Israel (Gerrity et al., 2010). The non-thermal process achieved near complete degradation of carbamazepine and meprobamate, suggesting that plasma-based technology is a viable alternative to the UV/H₂O₂ and O₃/H₂O₂ AOPs, especially considering the lower chemical requirements (Gerrity et al., 2010). A 200-L pilot plant with a plasma-assisted AOP was implemented to treat 18 µg L⁻¹ 1,4-dioxane (solvent), 30 µg L⁻¹ trichloroethylene (solvent), and 87 µg L⁻¹ N-nitrosodimethylamine (disinfection byproduct) in tertiary wastewater effluent. The plasma-assisted AOP attained 90% transformation of the three contaminants and outperformed the UV/H₂O₂ system, which recorded negligible degradation (Even-Ezra et al., 2009). These results suggest that plasma-based technologies exhibit major advantages over currently employed AOP systems. However, the application of plasma-assisted AOPs for treatment of contaminants of emerging concern in wastewater requires high electrical energy and skilled labor. Future efforts are, therefore, required to optimize the electrical energy requirements of plasma-assisted AOPs to facilitate sustainable application in wastewater treatment.

11. Summary

Throughout the last decade, a large number of review articles have addressed the mechanisms, kinetics, performance, and application of AOPs for wastewater treatment. However, few articles focused on the commercialization and full-scale implementation of AOPs to treat contaminants of emerging concern. This critical review comprehensively described the principles, advantages, disadvantages, and scale-up status of seven different categories of emerging AOP technologies. The modified-Fenton, photo-Fenton, ozonation, and heterogeneous catalysis AOPs have been well investigated, whereas the PMS, PS, US, gamma radiation, and plasma-based AOPs are more novel and less explored. Summaries of the advantages, disadvantages, and economics of different pilot- and field-scale AOPs are provided in Table 4 and Table 5, respectively.

From the above discussion, the gamma radiation, modified electrochemical oxidation, and plasma-assisted AOPs demonstrated a strong potential for pilot- and full-scale applications in wastewater treatment. The production of a variety of reactive radicals in the gamma radiation and plasma-assisted AOPs can provide effective treatment of a wide spectrum of contaminants of emerging concern without generating toxic secondary intermediates. The modified electrochemical AOP is also attracting great attention due to *in situ* production of H₂O₂, which can reduce the cost and risks associated with transportation, handling, and storage of concentrated H₂O₂. Furthermore, modified electrochemical oxidation processes are easy to operate, work over a wide pH range (unlike, Fenton oxidation and cavitation), and do not produce large volumes of sludge. The other emerging AOPs, including sulphate radical, catalytic ozonation, cavitation, and modified Fenton processes, are also promising, but further studies are needed to improve understanding of the corresponding reaction kinetics in complex wastewater matrices.

12. Conclusion

This critical review explored state-of-the-art AOP technologies and their application for treatment of contaminants of emerging concern.

Table 4

The main advantages and disadvantages of emerging AOPs.

AOP	Advantages	Disadvantages
Sulphate radical	<ul style="list-style-type: none"> • SO₄^{•-} have a half-life of 30–40 µs, which is more than three orders of magnitude longer than •OH (20 ns) • SO₄^{•-} work over a wide pH range (2.0–8.0) 	<ul style="list-style-type: none"> • Increases the salt content and presence of sulphate ions as end products • Depends upon energy or light sources like heat, UV, and US
Catalytic ozonation	<ul style="list-style-type: none"> • More effective than O₃ (alone) • Higher yield of •OH radicals • No pH restrictions 	<ul style="list-style-type: none"> • Catalysts are costly • Separation of catalysts is challenging • O₃ may produce toxic byproducts • Metal ion leaching • Difficult to regenerate and reuse catalysts
Cavitation	<ul style="list-style-type: none"> • Simple and flexible operation • Easy to handle • Minimal maintenance costs • Energy use is similar to UV systems • Eliminates mass transfer limitations by creating microbubbles and turbulence in solution 	<ul style="list-style-type: none"> • Additional oxidants, such as H₂O₂ and O₃, may be required to improve performance • No full-scale applications exist, raising feasibility concerns • Requires expensive pumps and sonic transducers • More efficient under acidic pH
Gamma radiation	<ul style="list-style-type: none"> • Minimal organic byproduct formation • Inactivates pathogenic microorganisms • High penetrating potential compared to UV radiation • Produces •OH, H⁺, H₂O₂, e_{aq}⁻, and H₂ without chemical or catalyst addition • No sludge production • No pH restrictions • High degradation rates • In-situ production of H₂O₂ at cathode can reduce the cost and risks associated with handling, transportation, and storage of H₂O₂ • No sludge production • Requires less treatment time • Easy to operate • Advantageous for saline wastewater treatment 	<ul style="list-style-type: none"> • Requires skilled labor and protective equipment for operation • Energy- and cost-intensive process
Modified-electrochemical oxidation	<ul style="list-style-type: none"> • No sludge production • No pH restrictions • High degradation rates • In-situ production of H₂O₂ at cathode can reduce the cost and risks associated with handling, transportation, and storage of H₂O₂ • No sludge production • Requires less treatment time • Easy to operate • Advantageous for saline wastewater treatment 	<ul style="list-style-type: none"> • High cost of electrode materials • Electrode fouling • Generates disinfection byproducts
Modified-Fenton	<ul style="list-style-type: none"> • Low iron leaching • Low iron-laden sludge production • High •OH formation • Wide working pH range 	<ul style="list-style-type: none"> • High operational costs • No full-scale applications exist, raising feasibility concerns
Plasma-assisted	<ul style="list-style-type: none"> • No costly chemicals required • Least amount of byproduct formation • Produces a variety of reactive species 	<ul style="list-style-type: none"> • Needs a lot of electrical energy to generate reactive species • Requires skilled labor for operation

Promising laboratory-scale results have been reported for emerging AOPs, but few scale-up trials have been conducted. The major challenge for implementation of full-scale AOPs is the high operating costs; therefore, technoeconomic assessments are needed to determine which AOPs are most feasible for scale-up and operation with real wastewater. Continuous improvements are also required to optimize reactor design and configuration, employ solar radiation instead of UV light, develop waste-derived catalysts, and improve reuse of catalytic materials. These developments will facilitate adoption of sustainable AOPs that improve

Table 5

Summary of cost estimations for wastewater treatment with selected AOPs.

Process	Contaminants	Reactor volume (L)	Operating conditions	Time (min)	Efficiency (%)	Energy required (kJ L ⁻¹)	Total operating cost (\$ m ⁻³)	Reference
Solar photocatalysis	Eight pesticides	150	ZnO = 200 mg L ⁻¹ S ₂ O ₈ ²⁻ = 150 mg L ⁻¹	240	90 (TOC)	n.a. ^a	29.75	Fenoll et al. (2012)
UV/PS	Trimethoprim	39	TiO ₂ = 200 mg L ⁻¹ humic acid = 10 mg L ⁻¹ PS = 0.125 mM	50	~100	9	n.a. ^a	Grilla et al. (2019)
US/H ₂ O ₂ /CuO	Phenol	7	US = 25 kHz CuO = 1.5 g L ⁻¹ H ₂ O ₂ = 2 g L ⁻¹	90	n.a. ^a	206.3	n.a. ^a	Khokhawala and Gogate (2011)
O ₃ /UV/H ₂ O ₂	Winery wastewater	9	H ₂ O ₂ = 1 g L ⁻¹	300	40 (TOC)	n.a. ^a	13.49	Lucas et al. (2010)
Solar/Fe ²⁺ /H ₂ O ₂	Antipyrine	35	S ₂ O ₈ ²⁻ = 50 mg L ⁻¹	180	90 (TOC)	2.64	0.44	Miralles-Cuevas et al. (2017)
solar/Fe ²⁺ /S ₂ O ₈ ²⁻	Caffeine		H ₂ O ₂ = 50 mg L ⁻¹			2.56	0.76	
UV/H ₂ O ₂	Carbamazepine					0.28	0.45	
UV/S ₂ O ₈ ²⁻	Ciprofloxacin					0.24	0.52	
Photo-Fenton	Sulfamethoxazole	50	Fe ²⁺ = 20 mg L ⁻¹	258	40 (TOC)	20.8	2.02	Sánchez Pérez et al. (2013)
	Oxamyl							
	Pyrimethanil							
	Methomyl							
	Dimethoate							
	Imidacloprid							
Visible light photocatalysis	4-chlorophenol	100	H ₂ O ₂ = 2.5 mmol L ⁻¹ h ⁻¹ ZnPC = 0.01 mmol L ⁻¹	300	29 (TOC) 100 (TOC)	n.a. ^a	12.66 2.06	Krystynik et al. (2014)
UV/H ₂ O ₂								
Catalytic ozonation	Coking wastewater	222,000	Mn _x Ce _{1-x} O ₂ / γ-Al ₂ O ₃ = 180 g L ⁻¹ O ₃ = 80 mg L ⁻¹	90	45.6 (COD)	n.a. ^a	0.27	He et al. (2020a, 2020b)

a: n.a., not available; b: € values converted to \$ from the data supplied in the article; \$ 1.00 = 0.93 €.

water quality and protect both human and ecological health.

Declaration of competing interest

The authors declare that they have no known competing financial interests or personal relationships that could have appeared to influence the work reported in this paper.

Acknowledgement

The present research work was funded by Department of Science and Technology, Government of India (File No. DST/TMD (EWO)/OWUIS-2018/RS-10). In addition, authors wants to acknowledge CSIR-Central Leather Research Institute with corresponding communication No. A/2022/EED/DST/1683.

Appendix A. Supplementary data

Supplementary data to this article can be found online at <https://doi.org/10.1016/j.jenvman.2022.115295>.

References

- Abdelsalam, M.E., Birkin, P.R., 2002. A study investigating the sonoelectrochemical degradation of an organic compound employing Fenton's reagent. *Phys. Chem. Chem. Phys.* 4, 5340–5345. <https://doi.org/10.1039/b205987h>.
- Abedi, K., Ghorbani-Shahna, F., Jaleh, B., Bahrami, A., Yarahmadi, R., Haddadi, R., Gandomi, M., 2015. Decomposition of chlorinated volatile organic compounds (CVOs) using NTP coupled with TiO₂/GAC, ZnO/GAC, and TiO₂-ZnO/GAC in a plasma-assisted catalysis system. *J. Electroanal. Chem.* 73, 80–88. <https://doi.org/10.1016/j.elstat.2014.10.008>.
- Adak, A., Das, I., Mondal, B., Koner, S., Datta, P., Blaney, L., 2019. Degradation of 2,4-dichlorophenoxyacetic acid by UV 253.7 and UV-H₂O₂: reaction kinetics and effects of interfering substances. *Emerg. Contam.* 5, 53–60. <https://doi.org/10.1016/j.emcon.2019.02.004>.
- Adak, A., Mangalgi, K.P., Lee, J., Blaney, L., 2015. UV irradiation and UV-H₂O₂ advanced oxidation of the roxarsone and nitarsone organoarsenicals. *Water Res.* 70, 74–85. <https://doi.org/10.1016/j.watres.2014.11.025>.
- Ahmadi, M., Jaafarzadeh Haghighifard, N., Darvishi Cheshmeh Soltani, R., Tobeishi, M., Jorfi, S., 2019. Treatment of a saline petrochemical wastewater containing recalcitrant organics using electro-Fenton process: persulfate and ultrasonic intensification. *Desalin. Water Treat.* 169, 241–250. <https://doi.org/10.5004/dwt.2019.24682>.
- Ahmadzadeh, S., Dolatabadi, M., 2018. Removal of acetaminophen from hospital wastewater using electro-fenton process. *Environ. Earth Sci.* 77, 53. <https://doi.org/10.1007/s12665-017-7203-7>.
- Al-Bsoul, A., Al-Shannag, M., Tawalbeh, M., Al-Taani, A.A., Lafi, W.K., Al-Othman, A., Alsheyab, M., 2020. Optimal conditions for olive mill wastewater treatment using ultrasound and advanced oxidation processes. *Sci. Total Environ.* 700, 134576. <https://doi.org/10.1016/j.scitotenv.2019.134576>.
- Al-Qaim, F.F., Mussa, Z.H., Othman, M.R., Abdullah, M.P., 2015. Removal of caffeine from aqueous solution by indirect electrochemical oxidation using a graphite-PVC composite electrode: a role of hypochlorite ion as an oxidising agent. *J. Hazard Mater.* 300, 387–397. <https://doi.org/10.1016/j.jhazmat.2015.07.007>.
- Alkharaji, T.S., 2019. Advanced oxidation process based on water radiolysis to degrade and mineralize diclofenac in aqueous solutions. *Sci. Total Environ.* 688, 708–717. <https://doi.org/10.1016/j.scitotenv.2019.06.164>.
- Alkharaji, T.S., Boukari, S.O.B., Alfidhl, F.S., 2017. Gamma irradiation-induced complete degradation and mineralization of phenol in aqueous solution: effects of reagent. *J. Hazard Mater.* 328, 29–36. <https://doi.org/10.1016/j.jhazmat.2017.01.004>.
- Anipsitakis, G.P., Dionysiou, D.D., 2003. Degradation of organic contaminants in water with sulfate radicals generated by the conjunction of peroxymonosulfate with cobalt. *Environ. Sci. Technol.* 37, 4790–4797. <https://doi.org/10.1021/es0263792>.
- Anpilov, A.M., Barkhudarov, E.M., Bark, Y.B., Zadiraka, Y.V., Christofi, M., Kozlov, Y.N., Kossyi, I.A., Kop'ev, V.A., Silakov, V.P., Taktakishvili, M.I., Temchin, S.M., 2001. Electric discharge in water as a source of UV radiation, ozone and hydrogen peroxide. *J. Phys. D Appl. Phys.* 34, 993–999. <https://doi.org/10.1088/0022-3727/34/6/322>.
- Antoniu, M.G., de la Cruz, A.A., Dionysiou, D.D., 2010. Degradation of microcystin-LR using sulfate radicals generated through photolysis, thermolysis and e⁻ transfer mechanisms. *Appl. Catal. B Environ.* 96, 290–298. <https://doi.org/10.1016/j.apcatb.2010.02.013>.
- Araujo, F.V.F., Yokoyama, L., Teixeira, L.A.C., Campos, J.C., 2011. Heterogeneous Fenton process using the mineral hematite for the discolouration of a reactive dye solution. *Braz. J. Chem. Eng.* 28, 605–616. <https://doi.org/10.1590/S0104-66322011000400006>.
- Argyle, M.D., Bartholomew, C.H., 2015. Heterogeneous catalyst deactivation and regeneration: a review. *Catalysts* 5, 145–269. <https://doi.org/10.3390/catal5010145>.
- Arimi, M.M., 2017. Modified natural zeolite as heterogeneous Fenton catalyst in treatment of recalcitrants in industrial effluent. *Prog. Nat. Sci. Mater. Int.* 27, 275–282. <https://doi.org/10.1016/j.pnsc.2017.02.001>.

- Arzate, S., Campos-Mañas, M.C., Miralles-Cuevas, S., Agüera, A., García Sánchez, J.L., Sánchez Pérez, J.A., 2020. Removal of contaminants of emerging concern by continuous flow solar photo-Fenton process at neutral pH in open reactors. *J. Environ. Manag.* 261, 110265. <https://doi.org/10.1016/j.jenvman.2020.110265>.
- Asghar, Asghar, Raman, Abdul Aziz Abdul, Daud, Wan Mohd Ashri Wan, 2015. Advanced oxidation processes for in-situ production of hydrogen peroxide/hydroxyl radical for textile wastewater treatment: a review. *J. Clean. Prod.* 87, 826–838. <https://doi.org/10.1016/j.jclepro.2014.09.010>.
- Ashokkumar, M., 2011. The characterization of acoustic cavitation bubbles – an overview. *Ultrason. Sonochem.* 18, 864–872. <https://doi.org/10.1016/j.ultsonch.2010.11.016>.
- Babu, S.G., Ashokkumar, M., Neppolian, B., 2016. The Role of ultrasound on advanced oxidation processes. *Top. Curr. Chem.* 374, 75. <https://doi.org/10.1007/s41061-016-0072-9>.
- Babunpusami, A., Muthukumar, K., 2014. A review on Fenton and improvements to the Fenton process for wastewater treatment. *J. Environ. Chem. Eng.* 2, 557–572. <https://doi.org/10.1016/j.jece.2013.10.011>.
- Bagal, M.V., Gogate, P.R., 2014. Wastewater treatment using hybrid treatment schemes based on cavitation and Fenton chemistry: a review. *Ultrason. Sonochem.* 21, 1–14. <https://doi.org/10.1016/j.ultsonch.2013.07.009>.
- Bagal, M.V., Gogate, P.R., 2013. Degradation of 2,4-dinitrophenol using a combination of hydrodynamic cavitation, chemical and advanced oxidation processes. *Ultrason. Sonochem.* 20, 1226–1235. <https://doi.org/10.1016/j.ultsonch.2013.02.004>.
- Bang, J.H., Suslick, K.S., 2010. Applications of ultrasound to the synthesis of nanostructured materials. *Adv. Mater.* 22, 1039–1059. <https://doi.org/10.1002/adma.200904093>.
- Barhoumi, N., Olvera-Vargas, H., Oturan, N., Huguenot, D., Gadri, A., Ammar, S., Brillas, E., Oturan, M.A., 2017. Kinetics of oxidative degradation/mineralization pathways of the antibiotic tetracycline by the novel heterogeneous electro-Fenton process with solid catalyst chalcophyrite. *Appl. Catal. B Environ.* 209, 637–647. <https://doi.org/10.1016/j.apcatb.2017.03.034>.
- Barik, A.J., Gogate, P.R., 2018. Hybrid treatment strategies for 2,4,6-trichlorophenol degradation based on combination of hydrodynamic cavitation and AOPs. *Ultrason. Sonochem.* 40, 383–394. <https://doi.org/10.1016/j.ultsonch.2017.07.029>.
- Beltrán, F.J., Rivas, F.J., Montero-de-Espinosa, R., 2003. Ozone-enhanced oxidation of oxalic acid in water with cobalt catalysts. 1. Homogeneous Catalytic Ozonation. *Ind. Eng. Chem. Res.* 42, 3210–3217. <https://doi.org/10.1021/ie0209982>.
- Blaney, L., Lawler, D.F., Katz, L.E., 2019. Transformation kinetics of cyclophosphamide and ifosfamide by ozone and hydroxyl radicals using continuous oxidant addition reactors. *J. Hazard Mater.* <https://doi.org/10.1016/j.jhazmat.2018.09.075>.
- Bogaerts, A., Neyts, E., Gijbels, R., van der Mullen, J., 2002. Gas discharge plasmas and their applications. *Spectrochim. Acta Part B At. Spectrosc.* 57, 609–658. [https://doi.org/10.1016/S0584-8547\(01\)00406-2](https://doi.org/10.1016/S0584-8547(01)00406-2).
- Brillas, E., Sirés, I., 2015. Electrochemical removal of pharmaceuticals from water streams: reactivity elucidation by mass spectrometry. *TrAC Trends Anal. Chem.* 70, 112–121. <https://doi.org/10.1016/j.trac.2015.01.013>.
- Cabrera Reina, A., Miralles-Cuevas, S., Cornejo, L., Pomares, L., Polo, J., Oller, I., Malato, S., 2020. The influence of location on solar photo-Fenton: process performance, photoreactor scaling-up and treatment cost. *Renew. Energy* 145, 1890–1900. <https://doi.org/10.1016/j.renene.2019.07.113>.
- Cai, J., Zhou, M., Liu, Y., Savall, A., Groenen Serrano, K., 2018. Indirect electrochemical oxidation of 2,4-dichlorophenoxyacetic acid using electrochemically-generated persulfate. *Chemosphere* 204, 163–169. <https://doi.org/10.1016/j.chemosphere.2018.04.004>.
- Çalışkan, Y., Yatmaz, H.C., Bektaş, N., 2017. Photocatalytic oxidation of high concentrated dye solutions enhanced by hydrodynamic cavitation in a pilot reactor. *Process Saf. Environ. Protect.* 111, 428–438. <https://doi.org/10.1016/j.psep.2017.08.003>.
- Capodaglio, A.G., 2020. Critical perspective on advanced treatment processes for water and wastewater: AOPs, ARPs, and AORPs. *Appl. Sci.* 10 <https://doi.org/10.3390/app10134549>.
- Casado, J., Fornaguera, J., Galán, M.I., 2006. Pilot scale mineralization of organic acids by electro-Fenton® process plus sunlight exposure. *Water Res.* 40, 2511–2516. <https://doi.org/10.1016/j.watres.2006.04.047>.
- Casierra-Martínez, H.A., Madera-Parra, C.A., Vargas-Ramírez, X.M., Caselles-Osorio, A., Torres-López, W.A., 2020. Diclofenac and carbamazepine removal from domestic wastewater using a constructed wetland-solar photo-Fenton coupled system. *Ecol. Eng.* 153, 105699. <https://doi.org/10.1016/j.ecoleng.2019.105699>.
- Changotra, R., Rajput, H., Paul Guin, J., Varshney, L., Dhir, A., 2019. Hybrid coagulation, gamma irradiation and biological treatment of real pharmaceutical wastewater. *Chem. Eng. J.* 370, 595–605. <https://doi.org/10.1016/j.cej.2019.03.256>.
- Chen, S., Blaney, L., Chen, P., Deng, S., Hopanna, M., Bao, Y., Yu, G., 2019. Ozonation of the 5-fluorouracil anticancer drug and its prodrug capecitabine: reaction kinetics, oxidation mechanisms, and residual toxicity. *Front. Environ. Sci. Eng.* 13 <https://doi.org/10.1007/s11783-019-1143-2>.
- Chmielewski, A.G., 2006. Application of ionizing radiation to environment protection. *ChemInform* 37, 17–24. <https://doi.org/10.1002/chin.200627276>.
- Choi, J., Cui, M., Lee, Y., Ma, J., Kim, J., Son, Y., Khim, J., 2019. Hybrid reactor based on hydrodynamic cavitation, ozonation, and persulfate oxidation for oxalic acid decomposition during rare-earth extraction processes. *Ultrason. Sonochem.* 52, 326–335. <https://doi.org/10.1016/j.ultsonch.2018.12.004>.
- Chowdhury, P., Viraraghavan, T., 2009. Sonochemical degradation of chlorinated organic compounds, phenolic compounds and organic dyes – a review. *Sci. Total Environ.* 407, 2474–2492. <https://doi.org/10.1016/j.scitotenv.2008.12.031>.
- Cuerda-Corraea, E.M., Alexandre-Franco, M.F., Fernández-González, C., 2019. Advanced oxidation processes for the removal of antibiotics from water. An Overview. *Water* 12, 102. <https://doi.org/10.3390/w12010102>.
- Cui, C., Jin, L., Jiang, L., Han, Q., Lin, K., Lu, S., Zhang, D., Cao, G., 2016. Removal of trace level amounts of twelve sulfonamides from drinking water by UV-activated peroxymonosulfate. *Sci. Total Environ.* 572, 244–251. <https://doi.org/10.1016/j.scitotenv.2016.07.183>.
- Dantas, T.L.P., Mendonça, V.P., José, H.J., Rodrigues, A.E., Moreira, R.F.P.M., 2006. Treatment of textile wastewater by heterogeneous Fenton process using a new composite Fe₂O₃/carbon. *Chem. Eng. J.* 118, 77–82. <https://doi.org/10.1016/j.cej.2006.01.016>.
- De Andrade, J.R., Vieira, M.G.A., da Silva, M.G.C., Wang, S., 2020. Oxidative degradation of pharmaceutical losartan potassium with N-doped hierarchical porous carbon and peroxymonosulfate. *Chem. Eng. J.* <https://doi.org/10.1016/j.cej.2019.122971>.
- De la Cruz, N., Esquiús, L., Grandjean, D., Magnet, A., Tungler, A., de Alencastro, L.F., Pulgarín, C., 2013. Degradation of emergent contaminants by UV, UV/H₂O₂ and neutral photo-Fenton at pilot scale in a domestic wastewater treatment plant. *Water Res.* 47, 5836–5845. <https://doi.org/10.1016/j.watres.2013.07.005>.
- Deng, D., Lin, X., Ou, J., Wang, Z., Li, S., Deng, M., Shu, Y., 2015. Efficient chemical oxidation of high levels of soil-sorbed phenanthrene by ultrasound induced, thermally activated persulfate. *Chem. Eng. J.* 265, 176–183. <https://doi.org/10.1016/j.cej.2014.12.055>.
- Deng, Y., Zhao, R., 2015. Advanced oxidation processes (AOPs) in wastewater treatment. *Curr. Pollut. Rep.* 1, 167–176. <https://doi.org/10.1007/s40726-015-0015-z>.
- Dong, C., Bao, Y., Sheng, T., Yi, Q., Zhu, Q., Shen, B., Xing, M., Lo, I.M.C., Zhang, J., 2021. Singlet oxygen triggered by robust bimetallic MoFe/TiO₂ nanospheres of highly efficacy in solar-light-driven peroxymonosulfate activation for organic pollutants removal. *Appl. Catal. B Environ.* 286, 119930. <https://doi.org/10.1016/j.apcatb.2021.119930>.
- Dos Santos, A.J., Sirés, I., Martínez-Huitle, C.A., Brillas, E., 2018. Total mineralization of mixtures of Tartrazine, Ponceau SS and Direct Blue 71 azo dyes by solar photoelectro-Fenton in pre-pilot plant. *Chemosphere* 210, 1137–1144. <https://doi.org/10.1016/j.chemosphere.2018.07.116>.
- Du, Y., Dai, M., Cao, J., Peng, C., Ali, I., Naz, I., Li, J., 2020. Efficient removal of acid orange 7 using a porous adsorbent-supported zero-valent iron as a synergistic catalyst in advanced oxidation process. *Chemosphere* 244, 125522. <https://doi.org/10.1016/j.chemosphere.2019.125522>.
- Duan, X., Sun, H., Kang, J., Wang, Y., Indrawirawan, S., Wang, S., 2015. Insights into heterogeneous catalysis of persulfate activation on dimensional-structured nanocarbons. *ACS Catal.* 5, 4629–4636. <https://doi.org/10.1021/acsatal.5b00774>.
- Duan, X., Yang, S., Wacławek, S., Fang, G., Xiao, R., Dionysiou, D.D., 2020. Limitations and prospects of sulfate-radical based advanced oxidation processes. *J. Environ. Chem. Eng.* 8, 103849. <https://doi.org/10.1016/j.jece.2020.103849>.
- Dular, M., Griessler-Bulc, T., Gutierrez-Aguirre, I., Heath, E., Kosjek, T., Krivograd Klemencić, A., Oder, M., Petkovšek, M., Rački, N., Ravnikar, M., Šarc, A., Širok, B., Zupanc, M., Žitnik, M., Kompare, B., 2016. Use of hydrodynamic cavitation in (waste)water treatment. *Ultrason. Sonochem.* 29, 577–588. <https://doi.org/10.1016/j.ultsonch.2015.10.010>.
- Even-Ezra, Itay, Mizrahi, Anat, Gerrity, Daniel, Snyder, Shane, Salvesson, Andrew, Lahav, Ori, 2009. Application of a novel plasma-based advanced oxidation process for efficient and cost-effective destruction of refractory organics in tertiary effluents and contaminated groundwater. *Desalin. Water Treat.* 11, 236–244. <https://doi.org/10.5004/dwt.2009.807>.
- Fast, S.A., Gude, V.G., Truax, D.D., Martin, J., Magbanua, B.S., 2017. A critical evaluation of advanced oxidation processes for emerging contaminants removal. *Environ. Process.* 4, 283–302. <https://doi.org/10.1007/s40710-017-0207-1>.
- Fenoll, J., Flores, P., Hellín, P., Martínez, C.M., Navarro, S., 2012. Photodegradation of eight miscellaneous pesticides in drinking water after treatment with semiconductor materials under sunlight at pilot plant scale. *Chem. Eng. J.* 204–205, 54–64. <https://doi.org/10.1016/j.cej.2012.07.077>.
- Fenton, H.J.H., 1894. Oxidation of tartaric acid in presence of iron. *J. Chem. Soc. Trans.* 65, 899–910. <https://doi.org/10.1039/CT8946500899>.
- Ferkous, H., Merouani, S., Hamdaoui, O., Pétrier, C., 2017. Persulfate-enhanced sonochemical degradation of naphthol blue black in water: evidence of sulfate radical formation. *Ultrason. Sonochem.* 34, 580–587. <https://doi.org/10.1016/j.ultsonch.2016.06.027>.
- Futakawa, M., Naoe, T., Tanaka, N., 2007. Visualization of mercury cavitation bubble collapse. In: *Experimental Analysis of Nano and Engineering Materials and Structures*. Springer Netherlands, Dordrecht, pp. 301–302. https://doi.org/10.1007/978-1-4020-6239-1_149.
- Gagol, M., Przyjazny, A., Boczkaj, G., 2018. Wastewater treatment by means of advanced oxidation processes based on cavitation – a review. *Chem. Eng. J.* 338, 599–627. <https://doi.org/10.1016/j.cej.2018.01.049>.
- Gagol, M., Soltani, R.D.C., Przyjazny, A., Boczkaj, G., 2019. Effective degradation of sulfide ions and organic sulfides in cavitation-based advanced oxidation processes (AOPs). *Ultrason. Sonochem.* 58, 104610. <https://doi.org/10.1016/j.ultsonch.2019.05.027>.
- Ganguli, A., Ganguly, P., Das, P., Saha, A., 2020. Integral approach for the treatment of phenolic wastewater using gamma irradiation and graphene oxide. *Groundw. Sustain. Dev.* 10, 100355. <https://doi.org/10.1016/j.gsd.2020.100355>.
- Ganiyu, S.O., Huang, L., T.X., Bechelany, M., Esposito, G., Van Hullebusch, E.D., Oturan, M.A., Cretin, M., 2017. A hierarchical CoFe-layered double hydroxide modified carbon-felt cathode for heterogeneous electro-Fenton process. *J. Mater. Chem.* 5, 3655–3666. <https://doi.org/10.1039/c6ta09100h>.

- Ganiyu, S.O., Zhou, M., Martínez-Huitle, C.A., 2018. Heterogeneous electro-Fenton and photoelectro-Fenton processes: a critical review of fundamental principles and application for water/wastewater treatment. *Appl. Catal. B Environ.* 235, 103–129. <https://doi.org/10.1016/j.apcatb.2018.04.044>.
- García-Segura, S., Ocon, J.D., Chong, M.N., 2018. Electrochemical oxidation remediation of real wastewater effluents — a review. *Process Saf. Environ. Protect.* 113, 48–67. <https://doi.org/10.1016/j.psep.2017.09.014>.
- Gerrity, D., Stanford, B.D., Trenholm, R.A., Snyder, S.A., 2010. An evaluation of a pilot-scale nonthermal plasma advanced oxidation process for trace organic compound degradation. *Water Res.* 44, 493–504. <https://doi.org/10.1016/j.watres.2009.09.029>.
- Gevari, M.T., Abbasi, T., Niazi, S., Ghorbani, M., Koşar, A., 2020. Direct and indirect thermal applications of hydrodynamic and acoustic cavitation: a review. *Appl. Therm. Eng.* 171, 115065. <https://doi.org/10.1016/j.applthermaleng.2020.115065>.
- Ghanbari, F., Moradi, M., 2017. Application of peroxymonosulfate and its activation methods for degradation of environmental organic pollutants: Review. *Chem. Eng. J.* 310, 41–62. <https://doi.org/10.1016/j.cej.2016.10.064>.
- Ghauch, A., Baalbaki, A., Amasha, M., El Asmar, R., Tantawi, O., 2017. Contribution of persulfate in UV-254 nm activated systems for complete degradation of chloramphenicol antibiotic in water. *Chem. Eng. J.* 317, 1012–1025. <https://doi.org/10.1016/j.cej.2017.02.133>.
- Ghezziar, M.R., Abdelmalek, F., Belhadj, M., Benderdouche, N., Addou, A., 2007. Gliding arc plasma assisted photocatalytic degradation of anthraquinonic acid green 25 in solution with TiO₂. *Appl. Catal. B Environ.* 72, 304–313. <https://doi.org/10.1016/j.apcatb.2006.11.008>.
- Giwa, A., Yusuf, A., Balogun, H.A., Sambudi, N.S., Bilad, M.R., Adeyemi, I., Chakraborty, S., Curcio, S., 2021. Recent advances in advanced oxidation processes for removal of contaminants from water: a comprehensive review. *Process Saf. Environ. Protect.* 146, 220–256. <https://doi.org/10.1016/j.psep.2020.08.015>.
- Gotvaj, A.Z., Rozman, U., Antončić, T., Urbanc, T., Vrabel, M., Derco, J., 2021. Fe²⁺ and UV catalytically enhanced ozonation of selected environmentally persistent antibiotics. *Processes* 9, 1–17. <https://doi.org/10.3390/pr9030521>.
- Gozzi, F., Sirés, I., Thiam, A., de Oliveira, S.C., Junior, A.M., Brillas, E., 2017. Treatment of single and mixed pesticide formulations by solar photoelectro-Fenton using a flow plant. *Chem. Eng. J.* 310, 503–513. <https://doi.org/10.1016/j.cej.2016.02.026>.
- Grilla, E., Matthaiou, V., Frontistis, Z., Oller, I., Polo, I., Malato, S., Mantzavinos, D., 2019. Degradation of antibiotic trimethoprim by the combined action of sunlight, TiO₂ and persulfate: a pilot plant study. *Catal. Today* 328, 216–222. <https://doi.org/10.1016/j.cattod.2018.11.029>.
- Gu, L., Nie, J.-Y., Zhu, N., Wang, L., Yuan, H.-P., Shou, Z., 2012. Enhanced Fenton's degradation of real naphthalene dye intermediate wastewater containing 6-nitro-1-diazo-2-naphthol-4-sulfonic acid: a pilot scale study. *Chem. Eng. J.* 189–190, 108–116. <https://doi.org/10.1016/j.cej.2012.02.038>.
- Guan, K., Zhou, P., Zhang, J., Zhu, L., 2020. Synthesis and characterization of ZnO@RSDBC composites and their Photo-Oxidative degradation of Acid Orange 7 in water. *J. Mol. Struct.* 1203, 127425. <https://doi.org/10.1016/j.molstruc.2019.127425>.
- Guerra-Rodríguez, S., Rodríguez, E., Singh, D., Rodríguez-Chueca, J., 2018. Assessment of sulfate radical-based advanced oxidation processes for water and wastewater treatment: a review. *Water* 10, 1828. <https://doi.org/10.3390/w10121828>.
- Haber, F., Weiss, J., 1932. The Catalytic Decomposition of Hydrogen Peroxide by Iron Salts, vol. 147. Royal Society, pp. 332–351. <https://doi.org/10.1098/rspa.1934.0221>.
- Han, B., Ko, J., Kim, J., Kim, Y., Chung, W., Makarov, I.E., Ponomarev, A.V., Pikaev, A.K., 2002. Combined electron-beam and biological treatment of dyeing complex wastewater. *Pilot Plant Exp. Radiat. Phys. Chem.* 64, 53–59. [https://doi.org/10.1016/S0969-806X\(01\)00452-2](https://doi.org/10.1016/S0969-806X(01)00452-2).
- Han, B., Kyu, J., Kim, Y., Seung, J., Young, K., 2012. Operation of industrial-scale electron beam wastewater treatment plant. *Radiat. Phys. Chem.* 81, 1475–1478. <https://doi.org/10.1016/j.radphyschem.2012.01.030>.
- Hasan, N., Kim, S., Kim, M.S., Nguyen, N.T.T., Lee, C., Kim, J., 2020. Visible light-induced activation of peroxymonosulfate in the presence of ferric ions for the degradation of organic pollutants. *Separ. Purif. Technol.* 240, 116620. <https://doi.org/10.1016/j.seppur.2020.116620>.
- Hassan, H., Hameed, B.H., 2011. Fe-clay as effective heterogeneous Fenton catalyst for the decolorization of Reactive Blue 4. *Chem. Eng. J.* 171, 912–918. <https://doi.org/10.1016/j.cej.2011.04.040>.
- Hayati, F., Isari, A.A., Anvaripour, B., Fattahi, M., Kakavandi, B., 2020. Ultrasound-assisted photocatalytic degradation of sulfadiazine using MgO/CNT heterojunction composite: effective factors, pathway and biodegradability studies. *Chem. Eng. J.* 381, 122636. <https://doi.org/10.1016/j.cej.2019.122636>.
- He, C., Wang, J., Wang, C., Zhang, C., Hou, P., Xu, X., 2020a. Catalytic ozonation of bio-treated coking wastewater in continuous pilot- and full-scale system: efficiency, catalyst deactivation and in-situ regeneration. *Water Res.* 183, 116090. <https://doi.org/10.1016/j.watres.2020.116090>.
- He, D.Q., Zhang, Y.J., Pei, D.N., Huang, G.X., Liu, C., Li, J., Yu, H.Q., 2020b. Degradation of benzoic acid in an advanced oxidation process: the effects of reducing agents. *J. Hazard Mater.* 382, 121090. <https://doi.org/10.1016/j.jhazmat.2019.121090>.
- Hiller, R., Putterman, S.J., Barber, B.P., 1992. Spectrum of synchronous picosecond sonoluminescence. *Phys. Rev. Lett.* 69, 1182–1184. <https://doi.org/10.1103/PhysRevLett.69.1182>.
- Hitam, C.N.C., Jalil, A.A., 2020. A review on exploration of Fe₂O₃ photocatalyst towards degradation of dyes and organic contaminants. *J. Environ. Manag.* 258, 110050. <https://doi.org/10.1016/j.jenvman.2019.110050>.
- Hu, P., Long, M., 2016. Cobalt-catalyzed sulfate radical-based advanced oxidation: a review on heterogeneous catalysts and applications. *Appl. Catal. B Environ.* 181, 103–117. <https://doi.org/10.1016/j.apcatb.2015.07.024>.
- Huang, D., Chen, N., Zhu, C., Fang, G., Zhou, D., 2021. The overlooked oxidative dissolution of silver sulfide nanoparticles by thermal activation of persulfate: processes, mechanisms, and influencing factors. *Sci. Total Environ.* 760, 144504. <https://doi.org/10.1016/j.scitotenv.2020.144504>.
- Huang, J., Li, X., Ma, M., Li, D., 2017. Removal of di-(2-ethylhexyl) phthalate from aqueous solution by UV/peroxymonosulfate: influencing factors and reaction pathways. *Chem. Eng. J.* 314, 182–191. <https://doi.org/10.1016/j.cej.2016.12.095>.
- Huang, X., Xu, Y., Shan, C., Li, X., Zhang, W., Pan, B., 2016. Coupled Cu(II)-EDTA degradation and Cu(II) removal from acidic wastewater by ozonation: performance, products and pathways. *Chem. Eng. J.* 299, 23–29. <https://doi.org/10.1016/j.cej.2016.04.044>.
- Ikhlaq, A., Javed, F., Sohail, R., Kazmi, M., Rehman, A., Qi, F., 2021. Solar Photo-Catalytic ozonation on γ -alumina for the removal of dyes in wastewater. *Int. J. Environ. Sci. Technol.* 18, 1967–1974. <https://doi.org/10.1007/s13762-020-02940-5>.
- Iqbal, M., Bhatti, I.A., 2015. Gamma radiation/H₂O₂ treatment of a nonylphenol ethoxylates: degradation, cytotoxicity, and mutagenicity evaluation. *J. Hazard Mater.* 299, 351–360. <https://doi.org/10.1016/j.jhazmat.2015.06.045>.
- Isarain-Chávez, E., Rodríguez, R.M., Garrido, J.A., Arias, C., Centellas, F., Cabot, P.L., Brillas, E., 2010. Degradation of the beta-blocker propranolol by electrochemical advanced oxidation processes based on Fenton's reaction chemistry using a boron-doped diamond anode. *Electrochim. Acta* 56, 215–221. <https://doi.org/10.1016/j.electacta.2010.08.097>.
- Itikawa, Y., Mason, N., 2005. Cross sections for electron collisions with water molecules. *J. Phys. Chem. Ref. Data* 34, 1–22. <https://doi.org/10.1063/1.1799251>.
- Jamil, A., Bokhari, T.H., Iqbal, M., Bhatti, I.A., Zuber, M., Nisar, J., Masood, N., 2020. Gamma radiation and hydrogen peroxide based advanced oxidation process for the degradation of disperse dye in aqueous medium. *Z. Phys. Chem.* 234, 279–294. <https://doi.org/10.1515/zpch-2019-1384>.
- Javadi, R., Qazi, U.Y., 2019. Catalytic oxidation process for the degradation of synthetic dyes: an overview. *Int. J. Environ. Res. Publ. Health* 16, 1–27. <https://doi.org/10.3390/ijerph16112066>.
- Jiang, B., Zheng, J., Qiu, S., Wu, M., Zhang, Q., Yan, Z., Xue, Q., 2014. Review on electrical discharge plasma technology for wastewater remediation. *Chem. Eng. J.* 236, 348–368. <https://doi.org/10.1016/j.cej.2013.09.090>.
- Jing, L., Chen, B., Wen, D., Zheng, J., Zhang, B., 2017. Pilot-scale treatment of atrazine production wastewater by UV/O₃/ultrasound : factor effects and system optimization. *J. Environ. Manag.* 203, 182–190. <https://doi.org/10.1016/j.jenvman.2017.07.027>.
- Joshi, R.P., Thagard, S.M., 2013. Streamer-like electrical discharges in water: Part I. fundamental mechanisms. *Plasma Chem. Plasma Process.* 33, 1–15. <https://doi.org/10.1007/s1090-012-9425-5>.
- Joshi, S.M., Gogate, P.R., 2019. Sonochemistry Intensification of industrial wastewater treatment using hydrodynamic cavitation combined with advanced oxidation at operating capacity of 70 L. *Ultrason. Sonochem.* 52, 375–381. <https://doi.org/10.1016/j.ultsonch.2018.12.016>.
- Jyoti, K.K., Pandit, A.B., 2001. Water disinfection by acoustic and hydrodynamic cavitation. *Biochem. Eng. J.* 7, 201–212. [https://doi.org/10.1016/S1369-703X\(00\)00128-5](https://doi.org/10.1016/S1369-703X(00)00128-5).
- Kang, J.-W., Hoffmann, M.R., 1998. Kinetics and mechanism of the sonolytic destruction of methyl tert-butyl ether by ultrasonic irradiation in the presence of ozone. *Environ. Sci. Technol.* 32, 3194–3199. <https://doi.org/10.1021/es970874u>.
- Kaviya, S., 2020. Progression in Fenton Process for the Wastewater Treatment. *Green Methods for Wastewater Treatment*. In: Naushad, M., Rajendran, S., Lichtfouse, E. (Eds.), In: Environmental Chemistry for a Sustainable World. Springer Nature, Switzerland, pp. 87–120. <https://doi.org/10.1007/978-3-030-16427-0>.
- Khan, J.A., Sayed, M., Khan, S., Shah, N.S., Dionysiou, D.D., Boczkaj, G., 2020. Advanced oxidation processes for the treatment of contaminants of emerging concern. In: *Contaminants of Emerging Concern in Water and Wastewater*. Elsevier, pp. 299–365. <https://doi.org/10.1016/B978-0-12-813561-7.00009-2>.
- Khare, P., Patel, R.K., Sharan, S., Shankar, R., 2021. Recent trends in advanced oxidation process for treatment of recalcitrant industrial effluents. *Adv. Oxid. Process. Effl. Treat. Plants* 137–160. <https://doi.org/10.1016/B978-0-12-820101-6.00008-6>.
- Khokhawala, I.M., Gogate, P.R., 2011. Intensification of sonochemical degradation of phenol using additives at pilot scale operation. *Water Sci. Technol.* 63, 2547–2552. <https://doi.org/10.2166/wst.2011.532>.
- Kilic, M.Y., Abdelraheem, W.H., He, X., Kestioglu, K., Dionysiou, D.D., 2019. Photochemical treatment of tyrosol, a model phenolic compound present in olive mill wastewater, by hydroxyl and sulfate radical-based advanced oxidation processes (AOPs). *J. Hazard Mater.* 367, 734–742. <https://doi.org/10.1016/j.jhazmat.2018.06.062>.
- Komineni, S., Zöckler, Jeffrey, Stocking, Andrew, Liang, Sun, Flores, Amparo, Kavanaugh, Michael, Rodriguez, Rey, Browne, Tom, Ruth, Roberts, Brown, Anthony, Stocking, Andrew, 2000. 3.0 Advanced oxidation processes. Center for Groundwater Restoration and Protection National Water Research Institute 111–208.
- Kovacic, A., Skufca, D., Zupanc, M., Gostiša, J., Bizjan, B., Kristofelc, N., Dolenc, M.S., Heath, E., 2020. The removal of bisphenols and other contaminants of emerging concern by hydrodynamic cavitation: from lab-scale to pilot-scale. *Sci. Total Environ.* 743, 140724. <https://doi.org/10.1016/j.scitotenv.2020.140724>.
- Krishnan, R.Y., Manikandan, S., Subbaya, R., Biruntha, M., Govarthanan, M., Karmegam, N., 2021. Removal of emerging micropollutants originating from pharmaceuticals and personal care products (PPCPs) in water and wastewater by advanced oxidation processes: a review. *Environ. Technol. Innovat.* 23, 101757. <https://doi.org/10.1016/j.eti.2021.101757>.
- Krystynik, P., Kluson, P., Hejda, S., Buzek, D., Masin, P., Tito, D.N., 2014. Semi-pilot scale environment friendly photocatalytic degradation of 4-chlorophenol with

- singlet oxygen species-Direct comparison with H_2O_2 /UV-C reaction system. *Appl. Catal. B Environ.* 160–161, 506–513. <https://doi.org/10.1016/j.apcatb.2014.05.051>.
- Kumar, P. S., Kumar, M.S., Pandit, A. B., 2000. Experimental quantification of chemical effects of hydrodynamic cavitation. *Chem. Eng. Sci.* 55, 1633–1639. [https://doi.org/10.1016/S0009-2509\(99\)00435-2](https://doi.org/10.1016/S0009-2509(99)00435-2).
- Labiadh, L., Oturan, M.A., Panizza, M., Hamadi, N. Ben, Ammar, S., 2015. Complete removal of AHPs synthetic dye from water using new electro-fenton oxidation catalyzed by natural pyrite as heterogeneous catalyst. *J. Hazard Mater.* 297, 34–41. <https://doi.org/10.1016/j.jhazmat.2015.04.062>.
- Lan, R.J., Li, J.T., Sun, H.W., Su, W. Bin, 2012. Degradation of naproxen by combination of Fenton reagent and ultrasound irradiation: optimization using response surface methodology. *Water Sci. Technol.* 66, 2695–2701. <https://doi.org/10.2166/wst.2012.508>.
- Lauterborn, W., 1979. Optic cavitation. *J. Phys. Colloq.* 40, C8–C273. <https://doi.org/10.1051/jphyscol:1979847>.
- Lesage, O., Falk, L., Tatoulian, M., Mantovani, D., Ognier, S., 2013. Treatment of 4-chlorobenzoic acid by plasma-based advanced oxidation processes. *Chem. Eng. Process. Process Intensif.* 72, 82–89. <https://doi.org/10.1016/j.ccep.2013.06.008>.
- Liang, C., Bruell, C.J., 2008. Thermally activated persulfate oxidation of trichloroethylene: experimental investigation of reaction orders. *Ind. Eng. Chem. Res.* 47, 2912–2918. <https://doi.org/10.1021/ie070820l>.
- Lin, N., Gong, Y., Wang, R., Wang, Y., Zhang, X., 2022. Critical review of perovskite-based materials in advanced oxidation system for wastewater treatment: design, applications and mechanisms. *J. Hazard Mater.* 424, 127637. <https://doi.org/10.1016/j.jhazmat.2021.127637>.
- Liu, Y.-J., Hu, C.-Y., Lo, S.-L., 2019. Direct and indirect electrochemical oxidation of amine-containing pharmaceuticals using graphite electrodes. *J. Hazard Mater.* 366, 592–605. <https://doi.org/10.1016/j.jhazmat.2018.12.037>.
- Liu, Z., Zhang, L., Dong, F., Dang, J., Wang, K., Wu, D., Zhang, J., Fang, J., 2018. Preparation of ultrasmall goethite nanorods and their application as heterogeneous fenton reaction catalysts in the degradation of azo dyes. *ACS Appl. Nano Mater.* 1, 4170–4178. <https://doi.org/10.1021/acsanm.8b00930>.
- Lucas, M.S., Peres, J.A., Li Puma, G., 2010. Treatment of winery wastewater by ozone-based advanced oxidation processes (O_3 , O_3/UV and $\text{O}_3/\text{UV}/\text{H}_2\text{O}_2$) in a pilot-scale bubble column reactor and process economics. *Separ. Purif. Technol.* 72, 235–241. <https://doi.org/10.1016/j.seppur.2010.01.016>.
- Luo, T., Feng, H., Tang, L., Lu, Y., Tang, W., Chen, S., Yu, J., Xie, Q., Ouyang, X., Chen, Z., 2020. Efficient degradation of tetracycline by heterogeneous electro-Fenton process using Cu-doped Fe_2O_3 : mechanism and degradation pathway. *Chem. Eng. J.* 382, 122970. <https://doi.org/10.1016/j.cej.2019.122970>.
- Ma, H., Wang, B., 2006. Electrochemical pilot-scale plant for oil field produced wastewater by M/C/Fe electrodes for injection. *J. Hazard Mater.* 132, 237–243. <https://doi.org/10.1016/j.jhazmat.2005.09.043>.
- Ma, J., Chen, Y., Nie, J., Ma, L., Huang, Y., Li, L., Liu, Y., Guo, Z., 2018. Pilot-scale study on catalytic ozonation of bio-treated dyeing and finishing wastewater using recycled waste iron shavings as a catalyst. *Sci. Rep.* 8, 7555. <https://doi.org/10.1038/s41598-018-25761-6>.
- Ma, S., Kim, K., Chun, S., Moon, S.Y., Hong, Y., 2020. Plasma-assisted advanced oxidation process by a multi-hole dielectric barrier discharge in water and its application to wastewater treatment. *Chemosphere* 243, 125377. <https://doi.org/10.1016/j.chemosphere.2019.125377>.
- Ma, Y.S., Sung, C.F., 2010. Investigation of carboxylic acid decomposition by a combination of ultrasound and Fenton process. *Sustain. Environ. Res.* 20, 213–219.
- Mahdi-Ahmed, M., Chiron, S., 2014. Ciprofloxacin oxidation by UV-C activated peroxymonosulfate in wastewater. *J. Hazard Mater.* 265, 41–46. <https://doi.org/10.1016/j.jhazmat.2013.11.034>.
- Mahmoodi, N.M., Keshavarzi, S., Oveisi, M., Rahimi, S., Hayati, B., 2019. Metal-organic framework (ZIF-8)/inorganic nanofiber (Fe_2O_3) nanocomposite: green synthesis and photocatalytic degradation using LED irradiation. *J. Mol. Liq.* 291, 111333. <https://doi.org/10.1016/j.molliq.2019.111333>.
- Malik, S.N., Ghosh, P.C., Vaidya, A.N., Mudliar, S.N., 2020. Hybrid ozonation process for industrial wastewater treatment: principles and applications: a review. *J. Water Proc. Eng.* 35, 101193. <https://doi.org/10.1016/j.jwpe.2020.101193>.
- Malvestiti, J.A., Cruz-Alcalde, A., López-Vinent, N., Dantas, R.F., Sans, C., 2019. Catalytic ozonation by metal ions for municipal wastewater disinfection and simultaneous micropollutants removal. *Appl. Catal. B Environ.* 259, 118104. <https://doi.org/10.1016/j.apcatb.2019.118104>.
- Manickam, S., Abidin, Z., Parthasarathy, S., Alzorqi, I., Huay, E., Joyce, T., Gomes, R.L., Ali, A., 2014. Role of H_2O_2 in the fluctuating patterns of COD (chemical oxygen demand) during the treatment of palm oil mill effluent (POME) using pilot scale triple frequency ultrasound cavitation reactor. *Ultrason. Sonochem.* 21, 1519–1526. <https://doi.org/10.1016/j.ultsonch.2014.01.002>.
- Martínez-Huitle, C.A., Ferro, S., 2006. Electrochemical oxidation of organic pollutants for the wastewater treatment: direct and indirect processes. *Chem. Soc. Rev.* 35, 1324–1340. <https://doi.org/10.1039/b517632h>.
- Mecha, A.C., Chollom, M.N., 2020. Photocatalytic ozonation of wastewater: a review. *Environ. Chem. Lett.* 18, 1491–1507. <https://doi.org/10.1007/s10311-020-01020-x>.
- Melo, R., Cabo Verde, S., Branco, J., Botelho, M.L., 2008. Gamma radiation induced effects on slaughterhouse wastewater treatment. *Radiat. Phys. Chem.* 77, 98–100. <https://doi.org/10.1016/j.radphyschem.2007.03.006>.
- Méndez-Arriaga, F., Torres-Palma, R.A., Pétrier, C., Esplugas, S., Gimenez, J., Pulgarin, C., 2009. Mineralization enhancement of a recalcitrant pharmaceutical pollutant in water by advanced oxidation hybrid processes. *Water Res.* 43, 3984–3991. <https://doi.org/10.1016/j.watres.2009.06.059>.
- Michael, I., Hapeshi, E., Michael, C., Varela, A.R., Kyriakou, S., Manaia, C.M., Fatta-Kassinos, D., 2012. Solar photo-Fenton process on the abatement of antibiotics at a pilot scale: degradation kinetics, ecotoxicity and phytotoxicity assessment and removal of antibiotic resistant enterococci. *Water Res.* 46, 5621–5634. <https://doi.org/10.1016/j.watres.2012.07.049>.
- Miklos, D.B., Remy, C., Jekel, M., Linden, K.G., Drewes, J.E., Hübner, U., 2018. Evaluation of advanced oxidation processes for water and wastewater treatment – a critical review. *Water Res.* 139, 118–131. <https://doi.org/10.1016/j.watres.2018.03.042>.
- Miller, C.J., Wadley, S., Waite, T.D., 2017. Fenton, photo-Fenton and Fenton-like processes. *Water Intell. Online* 16, 297–332. https://doi.org/10.2166/9781780407197_0297.
- Miralles-Cuevas, S., Darowna, D., Wanag, A., Mozia, S., Malato, S., Oller, I., 2017. Comparison of UV/ H_2O_2 , UV/ $\text{S}_2\text{O}_8^{2-}$, solar/ $\text{Fe(II)}/\text{H}_2\text{O}_2$ and solar/ $\text{Fe(II)}/\text{S}_2\text{O}_8^{2-}$ at pilot plant scale for the elimination of micro-contaminants in natural water: an economic assessment. *Chem. Eng. J.* 310, 514–524. <https://doi.org/10.1016/j.cej.2016.06.121>.
- Mishra, N., Reddy, R., Kuila, A., Rani, A., Nawaz, A., Pichiah, S., 2017. A review on advanced oxidation processes for effective water treatment. *Curr. World Environ.* 12, 469–489. <https://doi.org/10.12944/CWE.12.3.02>.
- Moradi, M., Elahinia, A., Vasseghian, Y., Dragoi, E.-N., Omid, F., Mousavi Khaneghah, A., 2020. A review on pollutants removal by Sono-photo-Fenton processes. *J. Environ. Chem. Eng.* 8, 104330. <https://doi.org/10.1016/j.jece.2020.104330>.
- Mota, A.L.N., Albuquerque, L.F., Beltrame, L.T.C., Chiavone-Filho Jr., O., A. M., Nascimento, C.A.O., 2009. Advanced oxidation processes and their application in the petroleum industry: a review. *Brazil. J. Pet. Gas* 2, 122–142.
- Murillo-Sierra, J.C., Ruiz-Ruiz, E., Hinojosa-Reyes, L., Guzmán-Mar, J.L., Machuca-Martínez, F., Hernández-Ramírez, A., 2018. Sulfamethoxazole mineralization by solar photo electro-Fenton process in a pilot plant. *Catal. Today* 313, 175–181. <https://doi.org/10.1016/j.cattod.2017.11.003>.
- Naji, T., Dirany, A., Carabin, A., Drogué, P., 2018. Large-scale disinfection of real swimming pool water by electro-oxidation. *Environ. Chem. Lett.* 16, 545–551. <https://doi.org/10.1007/s10311-017-0687-2>.
- Nakhate, P.H., Gadipelly, C.R., Joshi, N.T., Marathe, K.V., 2019. Engineering aspects of catalytic ozonation for purification of real textile industry wastewater at the pilot scale. *J. Ind. Eng. Chem.* 69, 77–89. <https://doi.org/10.1016/j.jiec.2018.09.010>.
- Nawaz, F., Cao, H., Xie, Y., Xiao, J., Chen, Y., Ghazi, Z.A., 2017. Selection of active phase of MnO_2 for catalytic ozonation of 4-nitrophenol. *Chemosphere* 168, 1457–1466. <https://doi.org/10.1016/j.chemosphere.2016.11.138>.
- Nidheesh, P.V., 2015. Heterogeneous Fenton catalysts for the abatement of organic pollutants from aqueous solution: a review. *RSC Adv.* 5, 40552–40577. <https://doi.org/10.1039/c5ra02023a>.
- Nidheesh, P.V., Gandhimathi, R., 2012. Trends in electro-Fenton process for water and wastewater treatment: an overview. *Desalination* 299, 1–15. <https://doi.org/10.1016/j.desal.2012.05.011>.
- Oturan, M.A., Aaron, J.J., 2014. Advanced oxidation processes in water/wastewater treatment: principles and applications. A review. *Crit. Rev. Environ. Sci. Technol.* <https://doi.org/10.1080/10643389.2013.829765>.
- Oturan, M.A., Brillas, E., 2007. Electrochemical advanced oxidation processes (EAOPs) for Environmental Applications. *Port. Electrochim. Acta* 25, 1–18. <https://doi.org/10.4152/pea.200701001>.
- Ouiriemi, I., Karrar, A., Oturan, N., Pazos, M., Rozales, E., Gadri, A., Sanromán, M.Á., Ammar, S., Oturan, M.A., 2017. Heterogeneous electro-Fenton using natural pyrite as solid catalyst for oxidative degradation of vanillic acid. *J. Electroanal. Chem.* 797, 69–77. <https://doi.org/10.1016/j.jelechem.2017.05.028>.
- Panda, D., Sethu, V., Manickam, S., 2020. Removal of hexabromocyclododecane using ultrasound-based advanced oxidation process: kinetics, pathways and influencing factors. *Environ. Technol. Innovat.* 17, 100605. <https://doi.org/10.1016/j.eti.2020.100605>.
- Papoutsakis, S., Miralles-Cuevas, S., Gondrexon, N., Baup, S., Malato, S., Pulgarin, C., 2015. Coupling between high-frequency ultrasound and solar photo-Fenton at pilot scale for the treatment of organic contaminants: an initial approach. *Ultrason. Sonochem.* 22, 527–534. <https://doi.org/10.1016/j.ultsonch.2014.05.003>.
- Pelegrini, R., Reyes, J., Durán, N., Zamora, P.P., De Andrade, A.R., 2000. Photoelectrochemical degradation of lignin. *J. Appl. Electrochem.* 30, 953–958. <https://doi.org/10.1023/A:1004007730721>.
- Pérez, T., Sirés, I., Brillas, E., Nava, J.L., 2017. Solar photoelectro-Fenton flow plant modeling for the degradation of the antibiotic erythromycin in sulfate medium. *Electrochim. Acta* 228, 45–56. <https://doi.org/10.1016/j.electacta.2017.01.047>.
- Pikalova, E.Y., Sadykov, V.A., Filonova, E.A., Ereemeev, N.F., Sadovskaya, E.M., Pikalov, S.M., Bogdanovich, N.M., Lyagaeva, J.G., Kolchugin, A.A., Vedmid, L.B., Ishchenko, A.V., Goncharov, V.B., 2019. Structure, oxygen transport properties and electrode performance of Ca-substituted Ni_2NiO_4 . *Solid State Ionics* 335, 53–60. <https://doi.org/10.1016/j.ssi.2019.02.012>.
- Pines, D.S., Reckhow, D.A., 2002. Effect of dissolved cobalt(II) on the ozonation of oxalic acid. *Environ. Sci. Technol.* 36, 4046–4051. <https://doi.org/10.1021/es011230w>.
- Pirgalioglu, S., Özbelge, T.A., 2009. Comparison of non-catalytic and catalytic ozonation processes of three different aqueous single dye solutions with respect to powder copper sulfide catalyst. *Appl. Catal. Gen.* 363, 157–163. <https://doi.org/10.1016/j.apcata.2009.05.011>.
- Pliego, G., Zazo, J.A., García-Muñoz, P., Muñoz, M., Casas, J.A., Rodríguez, J.J., 2015. Trends in the intensification of the Fenton process for wastewater treatment: an overview. *Crit. Rev. Environ. Sci. Technol.* 45, 2611–2692. <https://doi.org/10.1080/10643389.2015.1025646>.

- Pourehie, O., Saïen, J., 2020. Homogeneous solar Fenton and alternative processes in a pilot-scale rotatable reactor for the treatment of petroleum refinery wastewater. *Process Saf. Environ. Protect.* <https://doi.org/10.1016/j.psep.2020.01.006>.
- Poyatos, J.M., Muñoz, M.M., Almerica, M.C., Torres, J.C., Hontoria, E., Osorio, F., 2010. Advanced oxidation processes for wastewater treatment: state of the art. *Water Air Soil Pollut.* 205, 187–204. <https://doi.org/10.1007/s11270-009-0065-1>.
- Pradhan, A.A., Gogate, P.R., 2010. Removal of p-nitrophenol using hydrodynamic cavitation and Fenton chemistry at pilot scale operation, 156, pp. 77–82. <https://doi.org/10.1016/j.ccej.2009.09.042>.
- Priambodo, R., Shih, Y.J., Huang, Y.J., Huang, Y.H., 2011. Treatment of real wastewater using semi batch (Photo)-Electro-Fenton method. *Sustain. Environ. Res.* 21, 389–393.
- Priyadarshini, Monali, Ahmad, A., Das, S., Ghangrekar, M.M., 2021a. Application of microbial electrochemical technologies for the treatment of petrochemical wastewater with concomitant valuable recovery: a review. *Environ. Sci. Pollut. Res.* 1–20. <https://doi.org/10.1007/s11356-021-14944-w>.
- Priyadarshini, M., Ahmad, A., Das, S., Ghangrekar, M.M., 2021b. Metal organic frameworks as emergent oxygen-reducing cathode catalysts for microbial fuel cells: a review. *Int. J. Environ. Sci. Technol.* <https://doi.org/10.1007/s13762-021-03499-5>.
- Priyadarshini, M., Das, I., Ghangrekar, M.M., 2020. Application of metal organic framework in wastewater treatment and detection of pollutants: Review. *J. Indian Chem. Soc.* 97, 507–512.
- Qian, Y., Liu, X., Li, K., Gao, P., Chen, J., Liu, Z., Zhou, X., Zhang, Y., Chen, H., Li, X., Xue, G., 2020. Enhanced degradation of cephalosporin antibiotics by matrix components during thermally activated persulfate oxidation process. *Chem. Eng. J.* 384, 123332. <https://doi.org/10.1016/j.ccej.2019.123332>.
- Rahman, R.O.A., Hung, Y.-T., 2019. Application of ionizing radiation in wastewater treatment: an Overview. *Water* 12 (1), 19. <https://doi.org/10.3390/w12010019>.
- Rao, L., Yang, Y., Chen, L., Liu, X., Chen, H., Yao, Y., Wang, W., 2020. Highly efficient removal of organic pollutants via a green catalytic oxidation system based on sodium metaborate and peroxymonosulfate. *Chemosphere* 238, 124687. <https://doi.org/10.1016/j.chemosphere.2019.124687>.
- Ratshiedana, R., Kuvarega, A.T., Mishra, A.K., 2021. Titanium dioxide and graphitic carbon nitride-based nanocomposites and nanofibres for the degradation of organic pollutants in water: a review. *Environ. Sci. Pollut. Res.* 28, 10357–10374. <https://doi.org/10.1007/s11356-020-11987-3>.
- Rauf, M.A., Ashraf, S.S., 2009. Radiation induced degradation of dyes—an overview. *J. Hazard Mater.* 166, 6–16. <https://doi.org/10.1016/j.jhazmat.2008.11.043>.
- Rayaroth, M.P., Aravindakumar, C.T., Shah, N.S., Boczkaj, G., 2022. Advanced oxidation processes (AOPs) based wastewater treatment - unexpected nitration side reactions - a serious environmental issue: a review. *Chem. Eng. J.* 430, 133002. <https://doi.org/10.1016/j.ccej.2021.133002>.
- Reddy, P.M.K., Subrahmanyam, C., 2012. Green approach for wastewater treatment-degradation and mineralization of aqueous organic pollutants by discharge plasma. *Ind. Eng. Chem. Res.* 51, 11097–11103. <https://doi.org/10.1021/ie301122p>.
- Rehman, F., Sayed, M., Khan, J.A., Shah, N.S., Khan, H.M., Dionysiou, D.D., 2018. Oxidative removal of brilliant green by UV/S₂O₈²⁻, UV/HSO₅⁻ and UV/H₂O₂ processes in aqueous media: a comparative study. *J. Hazard Mater.* 357, 506–514. <https://doi.org/10.1016/j.jhazmat.2018.06.012>.
- Ribeiro, J.P., Marques, C.C., Portugal, I., Nunes, M.I., 2020. AOX removal from pulp and paper wastewater by Fenton and photo-Fenton processes: a real case-study. *Energy Rep.* 6, 770–775. <https://doi.org/10.1016/j.egyr.2019.09.068>.
- Rodríguez-Chueca, J., Laski, E., García-Canibano, C., Martín de Vidales, M.J., Encinas, Á., Kuch, B., Marugán, J., 2018. Micropollutants removal by full-scale UV-C/sulfate radical based Advanced Oxidation Processes. *Sci. Total Environ.* 630, 1216–1225. <https://doi.org/10.1016/j.scitotenv.2018.02.279>.
- Rodríguez-Chueca, J., Varella della Giustina, S., Rocha, J., Fernandes, T., Pablos, C., Encinas, Á., Barceló, D., Rodríguez-Mozaz, S., Manaia, C.M., Marugán, J., 2019. Assessment of full-scale tertiary wastewater treatment by UV-C based-AOPs: removal or persistence of antibiotics and antibiotic resistance genes? *Sci. Total Environ.* 652, 1051–1061. <https://doi.org/10.1016/j.scitotenv.2018.10.223>.
- Rodríguez, M., Malato, S., Pulgarin, C., Contreras, S., Curcó, D., Giménez, J., Esplugas, S., 2005. Optimizing the solar photo-Fenton process in the treatment of contaminated water. Determination of intrinsic kinetic constants for scale-up. *Sol. Energy* 79, 360–368. <https://doi.org/10.1016/j.solener.2005.02.024>.
- Rosenfeldt, E.J., Linden, K.G., Canonica, S., von Gunten, U., 2006. Comparison of the efficiency of OH radical formation during ozonation and the advanced oxidation processes O₃/H₂O₂ and UV/H₂O₂. *Water Res.* 40, 3695–3704. <https://doi.org/10.1016/j.watres.2006.09.008>.
- Ruppert, G., Bauer, R., Heisler, G., 1993. The photo-Fenton reaction - an effective photochemical wastewater treatment process. *J. Photochem. Photobiol. Chem.* 73, 75–78. [https://doi.org/10.1016/1010-6030\(93\)80035-8](https://doi.org/10.1016/1010-6030(93)80035-8).
- Sabri, M., Habibi-Yangjeh, A., Ghosh, S., 2020. Novel ZnO/CuBi₂O₄ heterostructures for persulfate-assisted photocatalytic degradation of dye contaminants under visible light. *J. Photochem. Photobiol. Chem.* 391, 112397. <https://doi.org/10.1016/j.jphotochem.2020.112397>.
- Salimi, M., Esrafil, A., Gholami, M., Jafari, A.J., Kalantary, R.R., Farzadkia, M., Kermani, M., Sobhi, H.R., 2017. Contaminants of emerging concern: a review of new approach in AOP technologies. *Environ. Monit. Assess.* 189, 414. <https://doi.org/10.1007/s10661-017-6097-x>.
- Sánchez Pérez, J.A., Román Sánchez, I.M., Carra, I., Cabrera Reina, A., Casas López, J.L., Malato, S., 2013. Economic evaluation of a combined photo-Fenton/MBR process using pesticides as model pollutant. Factors affecting costs. *J. Hazard Mater.* 244–245, 195–203. <https://doi.org/10.1016/j.jhazmat.2012.11.015>.
- Sánchez-Montes, Isaac, Pérez, José F., Sáez, Cristina, Rodrigo, Manuel A., Cañizares, Pablo, Aquino, José M., 2020. Assessing the performance of electrochemical oxidation using DSA® and BDD anodes in the presence of UVC light. *Chemosphere* 238 (Jan), 124575. <https://doi.org/10.1016/j.chemosphere.2019.124575>.
- Scholtz, V., Pazlarova, J., Soukova, H., Khun, J., Julak, J., 2015. Nonthermal plasma - a tool for decontamination and disinfection. *Biotechnol. Adv.* 33, 1108–1119. <https://doi.org/10.1016/j.biotechadv.2015.01.002>.
- Segura, Y., Molina, R., Martínez, F., Melero, J., 2009. Integrated heterogeneous sono-photo Fenton processes for the degradation of phenolic aqueous solutions. *Ultrason. Sonochem.* 16, 417–424. <https://doi.org/10.1016/j.ultsonch.2008.10.004>.
- Senthilnathan, J., Philip, L., 2010. Photocatalytic degradation of lindane under UV and visible light using N-doped TiO₂. *Chem. Eng. J.* 161, 83–92. <https://doi.org/10.1016/j.ccej.2010.04.034>.
- Silva, L.G.R., Costa, E.P., Starling, M.C.V.M., dos Santos Azevedo, T., Bottrel, S.E.C., Pereira, R.O., Sanson, A.L., Afonso, R.J.C.F., Amorim, C.C., 2021. LED irradiated photo-Fenton for the removal of estrogenic activity and endocrine disruptors from wastewater treatment plant effluent. *Environ. Sci. Pollut. Res.* 28, 24067–24078. <https://doi.org/10.1007/s11356-021-12359-1>.
- Sirés, I., Brillas, E., Oturan, M.A., Rodrigo, M.A., Panizza, M., 2014. Electrochemical advanced oxidation processes: today and tomorrow. A review. *Environ. Sci. Pollut. Res.* 21, 8336–8367. <https://doi.org/10.1007/s11356-014-2783-1>.
- Sivodia, C., Sinha, A., 2020. Assessment of graphite electrode on the removal of anticancer drug cytarabine via indirect electrochemical oxidation process: kinetics & pathway study. *Chemosphere* 243, 125456. <https://doi.org/10.1016/j.chemosphere.2019.125456>.
- Skoumal, M., Rodríguez, R.M., Cabot, P.L., Centellas, F., Garrido, J.A., Arias, C., Brillas, E., 2009. Electro-Fenton, UVA photoelectro-Fenton and solar photoelectro-Fenton degradation of the drug ibuprofen in acid aqueous medium using platinum and boron-doped diamond anodes. *Electrochim. Acta* 54, 2077–2085. <https://doi.org/10.1016/j.electacta.2008.07.014>.
- Staehelin, J., Holgné, J., 1982. Decomposition of ozone in water: rate of initiation by hydroxide ions and hydrogen peroxide. *Environ. Sci. Technol.* 16, 676–681. <https://doi.org/10.1021/es00104a009>.
- Sun, M., Lei, Y., Cheng, H., Ma, J., Qin, Y., Kong, Y., Komarneni, S., 2020. Mg doped CuO-Fe₂O₃ composites activated by persulfate as highly active heterogeneous catalysts for the degradation of organic pollutants. *J. Alloys Compd.* 825, 154036. <https://doi.org/10.1016/j.jallcom.2020.154036>.
- Tamimi, M., Qourzal, S., Assabbane, A., Chovelon, J.M., Ferronato, C., Ait-Ichou, Y., 2006. Photocatalytic degradation of pesticide methomyl: determination of the reaction pathway and identification of intermediate products. *Photochem. Photobiol. Sci.* 5, 477–482. <https://doi.org/10.1039/b517105a>.
- Telegan Chekem, C., Chiron, S., Mancaux, J.M., Plantard, G., Goetz, V., 2020. Thermal activation of persulfates for wastewater depollution on pilot scale solar equipment. *Sol. Energy* 205, 372–379. <https://doi.org/10.1016/j.solener.2020.04.075>.
- Thanekar, P., Garg, S., Gogate, P.R., 2020. Hybrid treatment strategies based on hydrodynamic cavitation, advanced oxidation processes, and aerobic oxidation for efficient removal of naproxen. *Ind. Eng. Chem. Res.* 59, 4058–4070. <https://doi.org/10.1021/acs.iecr.9b01395>.
- Thomas, N., Dionysiou, D.D., Pillai, S.C., 2021. Heterogeneous Fenton catalysts: A review of recent advances. *J. Hazard Mater.* 404, 124082. <https://doi.org/10.1016/j.jhazmat.2020.124082>.
- Tichonovas, M., Krugly, E., Jankunaite, D., Racys, V., Martuzevicius, D., 2017. Ozone-UV-catalysis based advanced oxidation process for wastewater treatment. *Environ. Sci. Pollut. Res.* 24, 17584–17597. <https://doi.org/10.1007/s11356-017-9381-y>.
- Titchou, F.E., Zazou, H., Afanga, H., El Gaayda, J., Ait Akbour, R., Nidheesh, P.V., Hamdani, M., 2021a. Removal of organic pollutants from wastewater by advanced oxidation processes and its combination with membrane processes. *Chem. Eng. Process. - Process Intensif.* 169, 108631. <https://doi.org/10.1016/j.ccep.2021.108631>.
- Titchou, F.E., Zazou, H., Afanga, H., Gaayda, J., El, Ait Akbour, R., Nidheesh, P.V., Hamdani, M., 2021b. An overview on the elimination of organic contaminants from aqueous systems using electrochemical advanced oxidation processes. *J. Water Proc. Eng.* 41, 102040. <https://doi.org/10.1016/j.jwpe.2021.102040>.
- Tufail, A., Price, W.E., Mohseni, M., Pramanik, B.K., Hai, F.I., 2021. A critical review of advanced oxidation processes for emerging trace organic contaminant degradation: mechanisms, factors, degradation products, and effluent toxicity. *J. Water Proc. Eng.* 40, 101778. <https://doi.org/10.1016/j.jwpe.2020.101778>.
- Vandenbroucke, A.M., Morent, R., De Geyter, N., Leys, C., 2011. Non-thermal plasmas for non-catalytic and catalytic VOC abatement. *J. Hazard Mater.* 195, 30–54. <https://doi.org/10.1016/j.jhazmat.2011.08.060>.
- Vinet, L., Zhedanov, A., 2011. Heterogeneous photocatalytic oxidation of in process cyanide and sulfite in aqueous solutions at semiconductor powders. *J. Phys. Math. Theor.* 44, 1689–1699. <https://doi.org/10.1088/1751-8113/44/8/085201>.
- Waclawek, S., Lutze, H.V., Grübel, K., Padil, V.V.T., Černík, M., Dionysiou, D.D., 2017. Chemistry of persulfates in water and wastewater treatment: a review. *Chem. Eng. J.* 330, 44–62. <https://doi.org/10.1016/j.ccej.2017.07.132>.
- Wang, J., Chen, H., 2020. Catalytic ozonation for water and wastewater treatment: recent advances and perspective. *Sci. Total Environ.* 704, 135249. <https://doi.org/10.1016/j.scitotenv.2019.135249>.
- Wang, J.L., Xu, L.J., 2012. Advanced oxidation processes for wastewater treatment: formation of hydroxyl radical and application. *Crit. Rev. Environ. Sci. Technol.* 42, 251–325. <https://doi.org/10.1080/10643389.2010.507698>.
- Wang, N., Zheng, T., Zhang, G., Wang, P., 2016. A review on Fenton-like processes for organic wastewater treatment. *J. Environ. Chem. Eng.* 4, 762–787. <https://doi.org/10.1016/j.jece.2015.12.016>.
- Wang, Y., Xue, Y., Zhang, C., 2020. Generation and application of reactive chlorine species by electrochemical process combined with UV irradiation: synergistic

- mechanism for enhanced degradation performance. *Sci. Total Environ.* 712, 136501. <https://doi.org/10.1016/j.scitotenv.2020.136501>.
- Wang, Yujing, Zhao, G., Chai, S., Zhao, H., Wang, Yanbin, 2013. Three-dimensional homogeneous ferrite-carbon aerogel: one pot fabrication and enhanced electro-Fenton reactivity. *ACS Appl. Mater. Interfaces* 5, 842–852. <https://doi.org/10.1021/am302437a>.
- Weber, T.J., 2002. Wastewater treatment. *Met. Finish.* 100, 781–797. [https://doi.org/10.1016/S0026-0576\(02\)82077-3](https://doi.org/10.1016/S0026-0576(02)82077-3).
- Woitschläger, D., Humpl, B., Koncar, M., Siebenhofer, M., 2013. Electrochemical oxidation of wastewater - opportunities and drawbacks. *Water Sci. Technol.* 68, 1173–1179. <https://doi.org/10.2166/wst.2013.366>.
- Wojnárovits, L., Takács, E., 2008. Irradiation treatment of azo dye containing wastewater: an overview. *Radiat. Phys. Chem.* 77, 225–244. <https://doi.org/10.1016/j.radphyschem.2007.05.003>.
- Wu, C.H., Kuo, C.Y., Chang, C.L., 2008. Homogeneous catalytic ozonation of C.I. Reactive Red 2 by metallic ions in a bubble column reactor. *J. Hazard Mater.* 154, 748–755. <https://doi.org/10.1016/j.jhazmat.2007.10.087>.
- Wu, D., Xia, K., Fang, C., Chen, X., Ye, Y., 2020a. Rapid removal of azophloxine via catalytic degradation by a novel heterogeneous catalyst under visible light. *Catalysts* 10, 1–16. <https://doi.org/10.3390/catal10010138>.
- Wu, J., Wang, B., Blaney, L., Peng, G., Chen, P., Cui, Y., Deng, S., Wang, Y., Huang, J., Yu, G., 2019. Degradation of sulfamethazine by persulfate activated with organo-montmorillonite supported nano-zero valent iron. *Chem. Eng. J.* 361, 99–108. <https://doi.org/10.1016/j.cej.2018.12.024>.
- Wu, J., Wang, B., Cagnetta, G., Huang, J., Wang, Y., Deng, S., Yu, G., 2020b. Nanoscale zero valent iron-activated persulfate coupled with Fenton oxidation process for typical pharmaceuticals and personal care products degradation. *Separ. Purif. Technol.* 239, 116534. <https://doi.org/10.1016/j.seppur.2020.116534>.
- Wu, Z., Zhang, G., Zhang, R., Yang, F., 2018. Insights into mechanism of catalytic ozonation over practicable mesoporous Mn-CeO_x/γ-Al₂O₃ Catalysts. *Ind. Eng. Chem. Res.* 57, 1943–1953. <https://doi.org/10.1021/acs.iecr.7b04516>.
- Xia, X., Zhu, F., Li, J., Yang, H., Wei, L., Li, Q., Jiang, J., Zhang, G., Zhao, Q., 2020. A review study on sulfate-radical-based advanced oxidation processes for domestic/industrial wastewater treatment: degradation, efficiency, and mechanism. *Front. Chem.* 8, 1–16. <https://doi.org/10.3389/fchem.2020.592056>.
- Xia, Z., Hu, L., 2018. Treatment of organics contaminated wastewater by ozone micro-nano-bubbles. *Water* 11, 55. <https://doi.org/10.3390/w11010055>.
- Xiao, Y., Zhang, L., Zhang, W., Lim, K.Y., Webster, R.D., Lim, T.T., 2016. Comparative evaluation of iodoacids removal by UV/persulfate and UV/H₂O₂ processes. *Water Res.* 102, 629–639. <https://doi.org/10.1016/j.watres.2016.07.004>.
- Xiong, X., Wang, B., Zhu, W., Tian, K., Zhang, H., 2018. A review on ultrasonic catalytic microbubbles ozonation processes: properties, hydroxyl radicals generation pathway and potential in application. *Catalysts* 9, 10. <https://doi.org/10.3390/catal9010010>.
- Xu, L.J., Chu, W., Graham, N., 2014. Degradation of di-n-butyl phthalate by a homogeneous sono-photo-Fenton process with in situ generated hydrogen peroxide. *Chem. Eng. J.* 240, 541–547. <https://doi.org/10.1016/j.cej.2013.10.087>.
- Yang, W., Zhou, M., Oturan, N., Bechelany, M., Cretin, M., Oturan, M.A., 2020. Highly efficient and stable Fe^{II}/Fe^{III} LDH carbon felt cathode for removal of pharmaceutical ofloxacin at neutral pH. *J. Hazard Mater.* 393, 122513. <https://doi.org/10.1016/j.jhazmat.2020.122513>.
- Yang, W., Zhou, M., Oturan, N., Li, Y., Oturan, M.A., 2019. Electrocatalytic destruction of pharmaceutical imatinib by electro-Fenton process with graphene-based cathode. *Electrochim. Acta* 305, 285–294. <https://doi.org/10.1016/j.electacta.2019.03.067>.
- Yosofi, Y., Mousavi, S.A., 2020. Sono-photo-fenton degradation of reactive black 5 from aqueous solutions: performance and kinetics. *Desalination Water Treat.* 174, 354–360. <https://doi.org/10.5004/dwt.2020.24843>.
- Yu, X., Sun, J., Li, G., Huang, Y., Li, Y., Xia, D., Jiang, F., 2020. Integration of *SO₄-based AOP mediated by reusable iron particles and a sulfidogenic process to degrade and detoxify Orange II. *Water Res.* 174, 115622. <https://doi.org/10.1016/j.watres.2020.115622>.
- Zampeta, C., Bertaki, K., Triantaphyllidou, I., Frontistis, Z., Vayenas, D.V., 2021. Treatment of real industrial-grade dye solutions and printing ink wastewater using a novel pilot-scale hydrodynamic cavitation reactor. *J. Environ. Manag.* 297, 113301. <https://doi.org/10.1016/j.jenvman.2021.113301>.
- Zhang, B.T., Zhang, Y., Teng, Y., Fan, M., 2015. Sulfate radical and its application in decontamination technologies. *Crit. Rev. Environ. Sci. Technol.* 45, 1756–1800. <https://doi.org/10.1080/10643389.2014.970681>.
- Zhang, M. hui, Dong, H., Zhao, L., Wang, D. xi, Meng, D., 2019. A review on Fenton process for organic wastewater treatment based on optimization perspective. *Sci. Total Environ.* 670, 110–121. <https://doi.org/10.1016/j.scitotenv.2019.03.180>.
- Zhang, T., Yang, Y., Gao, J., Li, X., Yu, H., Wang, N., Du, P., Yu, R., Li, H., Fan, X., Zhou, Z., 2020. Synergistic degradation of chloramphenicol by ultrasound-enhanced nanoscale zero-valent iron/persulfate treatment. *Separ. Purif. Technol.* 240, 116575. <https://doi.org/10.1016/j.seppur.2020.116575>.
- Zhang, Y., Zhao, Y.-G., Maqbool, F., Hu, Y., 2022. Removal of antibiotics pollutants in wastewater by UV-based advanced oxidation processes: influence of water matrix components, processes optimization and application: a review. *J. Water Proc. Eng.* 45, 102496. <https://doi.org/10.1016/j.jwpe.2021.102496>.
- Zhao, J., He, Y., Wang, F., Zheng, W., Huo, C., Liu, X., Jiao, H., Yang, Y., Li, Y., Wen, X., 2020. Suppressing metal leaching in a supported Co/SiO₂ catalyst with effective protectants in the hydroformylation reaction. *ACS Catal.* 10, 914–920. <https://doi.org/10.1021/acscatal.9b03228>.
- Zhu, B., Cheng, H., Qin, Y., Ma, J., Kong, Y., Komarneni, S., 2020. Copper sulfide as an excellent co-catalyst with K₂S₂O₈ for dye decomposition in advanced oxidation process. *Separ. Purif. Technol.* 233, 116057. <https://doi.org/10.1016/j.seppur.2019.116057>.